Target Organ Toxicology Series

Toxicology of the Lung

Third Edition

Editors

Donald E. Gardner, Ph.D.
Inhalation Toxicology Associates
Raleigh, North Carolina

James D. Crapo, M.D.
Executive Vice President—Academic Affairs
Chairman, Department of Medicine
National Jewish Medical and Research Center
Denver, Colorado

Roger O. McClellan, D.V.M.
President, Chemical Industry Institute of Toxicology Research
Triangle Park, North Carolina

1999

Toxicology of the Lung, 3rd ed.
Edited by D. E. Gardner et al.

18

Dosimetry of Particles in Laboratory Animals and Humans

Frederick J. Miller

Chemical Industry Institute of Toxicology, Research Triangle Park, North Carolina, USA

For most compounds, the database for assessing potential risk to humans largely comes from animal toxicological studies. Toxicologists and risk assessors are faced with a series of judgments in deciding whether to use the animal data and then with various extrapolations if the animal results are used. This review examines factors

Most material taken directly from a critical review manuscript entitled "Dosimetry of Particles in Laboratory Animals and Humans in Relationship to Issues Surrounding Lung Overload and Human Health Risk Assessment" prepared by Dr. Miller for an ILSI Risk Science Institute workshop held March 23 and 24, 1998, in Washington, DC.

governing the dosimetry of inhaled particles in laboratory animals and humans and how complex interactions among these factors influence the inhalability, deposition, and clearance of particles as well as their temporal translocation and retention within the body. In addition, some insights on issues surrounding dosimetry of inhaled, poorly soluble, nonfibrous, nongenotoxic particles of low toxicity (hereafter referred to as *poorly soluble particles* [PSPs]) are presented as they contribute to our understanding of the phenomenon of "lung overload."

The factors governing the dosimetry of particles can be broadly grouped into two categories, one dealing with the physicochemical properties of the particles and the other with species-specific factors such as airway structure, ventilatory level, and mucociliary and alveolar clearance rates. Although particle dissolution rate and chemical composition are important physicochemical properties for the toxicity of many particles, they are basically unimportant for the dosimetry of PSPs, such as carbon black, coal, diesel soot, talc, and titanium dioxide. Particle size, density, and distribution are important physical properties for the deposition of all types of particles.

For the purpose of this review, dosimetry refers to estimating or measuring the amount (mass, number, surface area, volume, etc.) of particles at specific target sites at a particular point in time. This encompasses both deposition, which is the process of removing particles in various regions of the respiratory tract during the breathing of particle-laden air, and clearance, which refers to the rates and routes by which deposited particles are removed from the respiratory tract. Typically, the term *retention* in particulate inhalation toxicology refers to the amount of particles (sometimes called *retained deposits*) present at specific respiratory tract sites, that is, the net difference between deposition and clearance processes.

Experimental data on the deposition of particles usually are obtained from exposures lasting minutes to at most a few hours. In contrast, clearance data are obtained by measurements made over days to many weeks during exposure and/or after the cessation of exposure. Estimates of retained deposits arise when body burden measurements are made serially with time as inhalation exposures are continued. Chronic exposures result in respiratory-tract burdens that continue to increase over time until the rate of deposition is offset by the rate of clearance, thereby resulting in a steady-state burden from that time on. Body burden patterns differ among species. Higher exposure levels lead to higher steady-state burdens (Fig. 1). Curve C* of Figure 1 illustrates the type of retained lung burden seen with excessively high exposures that lead to impairment of alveolar macrophage (AM)–mediated particle clearance resulting in "lung overload." The breakpoint at which retained lung burden of PSPs starts to depart from the steady-state curve (C of Fig. 1) is inversely related to the magnitude of the exposure concentration. Dust overloading of the lungs has been postulated to occur if the retained burden of PSPs exceeds 1 mg per gram of lung (Morrow, 1988, 1992).

MECHANISMS OF DEPOSITION

Laws of physics govern the transport of particles entrained in the air. Particle transport and physical properties of the particles combine to yield mechanisms by which

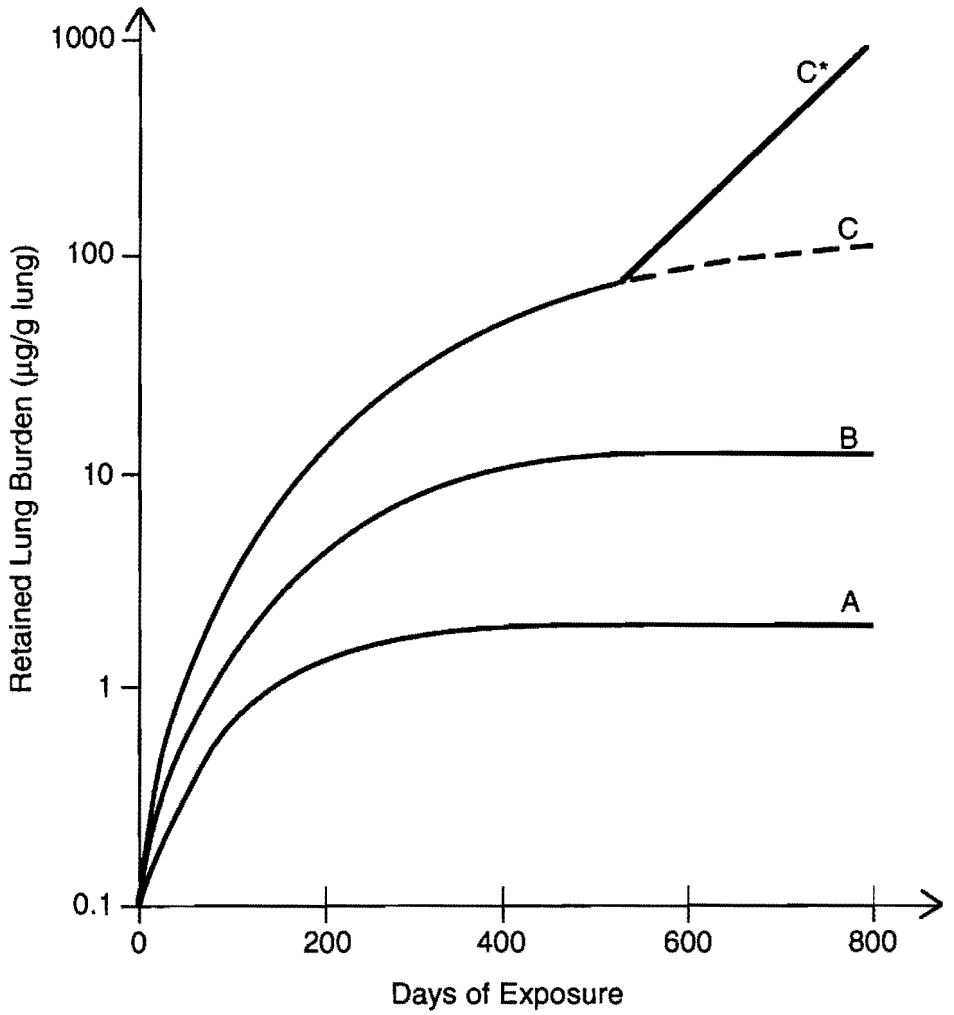

FIG. 1. Schematic representation of the relationship between retained lung burden and length of exposure leading to the phenomenon of lung overload. Curves A, B, and C are associated with progressively increasing exposure concentrations. If the exposure level is sufficiently high and the length of exposure sufficiently long, alveolar macrophage–mediated clearance of particles can be overwhelmed. If this occurs, retained lung burden increases linearly with further exposure (curve C*).

particles are removed from the airstream. The nature of the major mechanisms of deposition is described prior to discussion of the regions of the respiratory tracts of animals and humans in which the various mechanisms predominate.

The major mechanisms by which noncharged particles deposit are inertial impaction, sedimentation, and diffusion (Brownian). These mechanisms are illustrated schematically in Figure 2. Electrostatic attraction may be an important mechanism for the deposition of particles in some workplace exposure settings, if the processes being used generate charged particles and workers are in close proximity to the source of these particles. However, electrostatic attraction is not an important deposition mechanism for ambient exposures to particles, because there is ample time for such aerosols to come to Boltzman equilibrium. Inertial impaction is the process

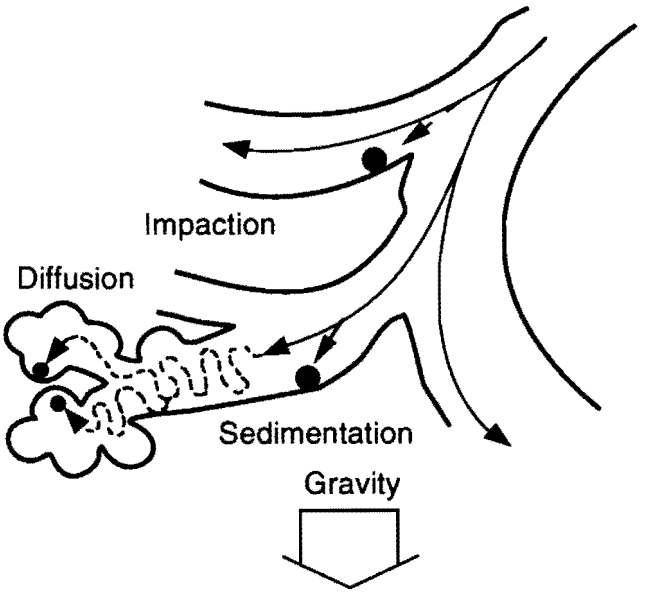

FIG. 2. Primary mechanisms of deposition of inhaled noncharged particles in the respiratory tract. *Solid lines*, streamline; *dashed lines*, particle trajectory. Modified from McClellan and Miller, (1997).

by which the inertia of the particle makes it unable to follow changes in the airstream direction or air velocity streamlines. *Sedimentation* refers to the settling out of particles from the airstream because of gravitational forces. The random displacement motion of particles resulting from constant bombardment by air molecules (Brownian diffusion) can result in particles coming into close proximity of airway surfaces. Depending upon particle size and airflow rate, diffusion, sedimentation, and impaction do not necessarily act as independent processes. Once particles are brought in close proximity to the airway walls, they are removed from the airstream by interception with the walls. Because objects that are relatively long compared with their diameters have an increased probability of the ends intercepting the wall of an airway, interception is often considered by some as a separate deposition mechanism for fibers.

The geometric (physical or diffusion equivalent) and aerodynamic equivalent diameters of a particle are important determinants of the relative importance of the mechanisms previously mentioned in the deposition of particles. Aerodynamic diameter (d_{ae}) takes into account the size, shape, and density of a particle and is defined to be the diameter of a unit density (1 g/cm^3) sphere having the same terminal settling velocity as the particle. Because particles of different sizes and density can have the same d_{ae}, they can be deposited in the same locations within the respiratory tract.

RESPIRATORY TRACT STRUCTURE AND FUNCTION

The respiratory tract can be subdivided into three main regions: the extrathoracic (ET) region (from the nose and mouth down to and including the larynx), the tracheobronchial tree (trachea to terminal bronchioles); and the pulmonary region (respiratory bronchioles to terminal alveolar sacs). Among disciplines, different

nomenclature often is used for these regions. For example, the upper respiratory tract is the same as the ET region; pulmonary and alveolar are used interchangeably. Also, the tracheobronchial (TB) region often is referred to as the *conducting airways.* The lower respiratory tract comprises the TB and A regions and is also referred to as the *thoracic region.* The anatomical or structural features of each of the major regions differ significantly among laboratory animals and humans on both macro- and microscopic scales. Table 1 provides a synopsis of key aspects of the morphology, cytology, histology, function, and structure of the respiratory tract of rats and humans. In the sections that follow, the structure and function of each region are briefly discussed, and some insights are provided as to which mechanisms of particle deposition are important in a given region.

ET Structure and Function

In the ET region, inhaled air is conditioned with respect to temperature and humidity (Proctor and Anderson, 1982), and there is an active mucociliary system for the removal of foreign solid material (Phipps, 1981). Similarities between rats and humans also extend to the cytology of the ET epithelium and the histology of the ET airway walls. The same four types of epithelium (squamous, transitional, respiratory, and olfactory) are present in both species, although the percentage of the ET covered by the types of epithelium differs among species (Harkema, 1992).

Probably the most significant differences in respiratory structure between rats and humans occur in the upper respiratory tract. Cross-sections of the nasal passages of these two species shown in Figure 3 illustrate the nature of the differences. Bulk airflow patterns are influenced by these complex structures such that major medial and lateral airflow streams are formed in the nose of the rat (Morgan et al., 1991; Kimbell et al., 1995) that are quite different from those in humans (Hahn et al., 1993; Subramaniam et al., 1998). The torturous nasal passages result in inertial impaction being the predominant mechanism by which inhaled particles larger than about 5 μm are deposited in the heads of both rats and humans. In addition, ultrafine particles (<0.1 μm in diameter) are effectively removed in the nose via diffusion, because the surfaces of the nasal turbinates are large compared to the cross-sectional area and are in close proximity to the inhaled air.

TB Structure and Function

The main function of the TB region of all mammalian species is to deliver oxygen efficiently to the alveolar region, where gas exchange (oxygen for carbon dioxide) occurs. The types of cells making up the TB epithelium are similar to those contained in the transitional and respiratory epithelium of the ET region. However, there are significant differences between rats and humans in the number of any given cell type as a function of airway size (Mercer, Russell, Roggli, and Crapo, 1994). The liquid layer lining the conducting airways contains mucus. This liquid

TABLE 1. *Key aspects of the structure and function of the respiratory tract of rats and humans*

Functions	Cytology (Epithelium)	Histology (Walls)	Anatomy	Zones (Air)	Location	Comments
Air conditioning: Temperature and Humidity, and Cleaning; Fast Particle Clearance; Air Conduction	Epithelium Types: Squamous Transitional Respiratory Olfactory Cell Types: Ciliated Cells Noncilliated Cells: Goblet Cells Mucous (Secretory) Cells Serous Cells Brush Cells Endocrine Cells Basal Cells Intermediate Cells	Mucous Membrane, Respiratory Epithelium (Pseudostratified, Ciliated, Mucous), Glands Mucous Membrane, Respiratory or Stratified Epithelium, Glands	Anterior Nasal Passages Nose Mouth Pharynx Posterior Larynx Esophagus	Conduction	Extrathoracic	Rats are obligate nasal breathers. Adult humans switch to oronasal breathing when minute ventilation exceeds about 35 Lmin^{-1} (Ninimaa et al., 1981)
		Mucous Membrane, Respiratory Epithelium Cartilage Rings, Glands	Trachea Main Bronchi		Thoracic / Tracheobronchial	
		Mucous Membrane, Respiratory Epithelium, Cartilage plates, Smooth Muscle Layer, Glands	Bronchi			Rat lung has predominantly a monopodial branching system (Crapo et al., 1990)
	Respiratory Epithelium With Clara Cells (No Goblet Cells) Cell Types: Ciliated Cells Noncilliated Cells: Clara (Secretory) Cells	Mucous Membrane, Respiratory Epithelium, No Cartilage, No Glands, Smooth Muscle Layer	Bronchioles			
		Mucous Membrane, Single-Layer Respiratory Epithelium, Less Ciliated, Smooth Muscle Layer	Terminal Bronchioles			
Air Conduction; Gas Exchange; Slow Particle Clearance	Respiratory Epithelium Consisting Mainly of Clara Cells (Secretory) and Few Ciliated Cells	Mucous Membrane, Single-Layer Respiratory Epithelium of Cuboidal Cells, Smooth Muscle Layer	Respiratory Bronchioles	Gas Exchange Transitory	Thoracic / Alveolar	
Gas Exchange; Very Slow Particle Clearance	Squamous Alveolar Epithelial Cells (Type I), Covering 94% of Alveolar Surface Areas Cuboidal Alveolar Epithelial Cells (Type II, Surfactant-Producing), Covering 6% of Alveolar Surface Area Alveolar Macrophages	Wall Consists of Alveolar Entrance Rings, Squamous Epithelial Layer, Surfactant	Alveolar Ducts			Rats do not have respiratory bronchioles. From the bronchiolar-alveolar duct junction in a rat, alveolar sacs are reached after anywhere from 3 to 13 branchings (Mercer & Crapo, 1987)
		Interalveolar Septa Covered by Squamous Epithelium, Containing Capillaries, Surfactant	Alveolar Sacs			
			Lymphatics			

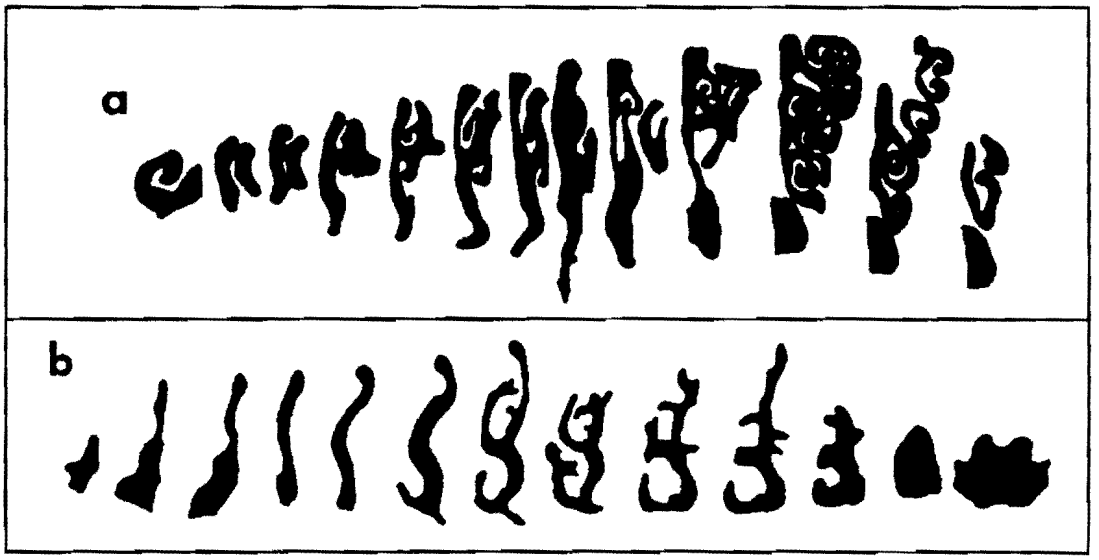

FIG. 3. Aspects of upper respiratory tract structure important for dosimetry. (*A*) Cross-sections of one side of the rat nasal passages, nostril at left. (*B*) Cross-sections of one side of the human nasal passages, nostril at left. From Miller and Kimbell (1995).

layer protects the tissue from direct exposure to inhaled pollutants and is composed of an epiphase and an underlying hypophase in which cilia beat in a manner that propels mucus to the glottis, where it is swallowed. For information on the comparative biochemistry of this layer, the reader is referred to work by Hatch (1992).

The thickness of the mucociliary layer varies as a function of location within the TB region. For rats and humans, Table 2 gives available data on the thickness of the liquid lining layer in the TB and ET regions and on mucous velocities. The mean mucous velocities given in Table 2 have associated with them relatively large standard deviations. As noted by Wolff (1992), clearance of mucus is not necessarily as relentless and uniform as one might be led to believe, particularly in view of the fact there are preferential routes of clearance. Thus, some deposited particles may be retained in areas of slow clearance for extended periods of time. The extent to which rats and humans may differ in this regard is not known. Observations in humans (Goodman et al., 1977) and in rats (Wolff et al., 1987) that mean tracheal mucous velocities decline with increasing age have important implications for assessing the risks of relatively insoluble particles, particularly if comparable reductions in mucociliary clearance also are occurring in smaller TB airways.

The structure of the TB region at the gross level can be thought of as a complex branching system of tubes or pipes. An anatomical depiction of the TB airways of humans corresponds to a symmetric branching system denoted as regular and dichotomous, because each branching parent tube gives rise to two daughter tubes of the same diameter. This corresponds to the lung model developed by Weibel (1963) and represents the lung structure that most often has been used in human dosimetry models for both gases and particles. In actuality, the conducting airways of humans

TABLE 2. *Extrathoracic and tracheobronchial liquid lining layer thickness and mucous velocities in humans and rats*

Species	Location	Thickness[a] (μm)	Comments	Reference	Mucous velocity (mm/min)	Reference
Human	Nose				5.2 ± 2.3 to 8.4 ± 4.8	van Ree et al., 1962; Andersen et al., 1971
	Trachea				3.6 ± 1.5 to 21.5 ± 5.5	Yeates et al., 1975; Santa Cruz et al., 1974
	Bronchi (main stem)	8.3[b]	Combination of airway and vascular fixation, lobes were surgical resections in nonsmokers (for methods, see Mercer and Crapo, 1987)	Mercer et al., 1992		
	Bronchi (segmental)	6.9[b]				
	Bronchioles	1.8[b]				
Rat	Nose	≤15	Observed a continuous blanket	Luchtel, 1976; Morgan et al., 1984	2.3 ± 0.8	Dahl et al., 1986
					1.1 to 5.9 (respiratory epithelium) 0.9 (olfactory epithelium)	Morgan et al., 1986
	Trachea, large bronchi	5–10 3–15,	"Distribution was focal"	Yoneda, 1976	1.9 ± 0.7 to 5.9 ± 2.5	Felicetti et al., 1981; Giordano and Morrow, 1972
	Trachea	generally 8–12[b]	Mucous blanket observed	Luchtel, 1978		
	Lobar bronchi	Few tenths–8, generally 2–5[b]				
	Trachea	6.1[b]	Combination of airway and vascular fixation (for methods, see Mercer and Crapo, 1987)	Mercer et al., 1992		
	Bronchi	3[b]				
	Bronchioles	2[b]				
	Terminal bronchioles; trachea, major bronchi, peripheral airways	0	No epiphase or mucus observed."Well defined streams up to 500 mm wide." "Mucus was transported as discrete particles" as small as 0.5 mm in diameter. A continuous mucous blanket was not observed.	Irvani and van As, 1972; Stephens et al., 1974; van As and Webster, 1972, 1974		

[a]Unless specified, values apply only to the epiphase above cilia tips.
[b]Thickness of epiphase plus hypophase.

exhibit an irregular bipodial and tripodial branching pattern (Crapo et al., 1990). Despite this, when Martonen (1983) compared the results obtained using symmetric TB geometries (Weibel, 1963; Soong et al., 1979) with the asymmetric model of Horsfield et al. (1971), he found that the symmetric models gave better agreement with the available human experimental deposition data than did the asymmetric model.

The TB airways in the rat lung have predominately a monopodial branching system (Crapo et al., 1990). In rats, terminal bronchioles can be reached after anywhere from 7 to 32 branchings, whereas the airways in each lobe of the human lung require about anywhere from 9 to 22 branchings to reach a terminal bronchiole (Yeh and Harkema, 1993). The difference between the TB airway branching systems of rodents and primates is illustrated schematically in Figure 4. The branching differences are particularly important relative to the sites of deposition of inhaled particles. Impaction is the predominant mechanism for particle deposition in the TB airways of humans for particles greater than 2.5 μm d_{ae}; both impaction and sedimentation are important for deposition of particles greater than 1 μm d_{ae} in the TB airways of laboratory animals. Because mean flow rate and residence time influence impaction and sedimentation, respectively, impaction is even more significant for TB deposition as humans engage in activities that increase their minute ventilation. In humans and rats, enhanced deposition of particles larger than 2.5 μm during inspiration occurs at airway bifurcations (Martonen and Hofmann, 1986; Schlesinger, 1989). With expiration, there is a tendency in humans for increased deposition on the walls of the parent tube within a distance of about one diameter of the airway size; the monopodial branching system of the rat tends to impart increased deposition on the parent wall opposite the opening of the smaller daughter airway (Schlesinger, 1989). Also, the turbulence created by the laryngeal jet tends to result in enhanced deposition of ultrafine particles (<0.1 μm in geometric diame-

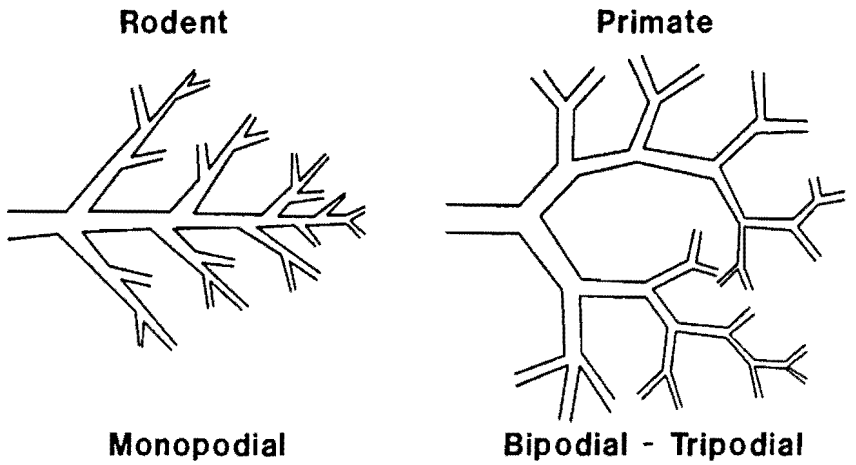

FIG. 4. Illustration of short and long pathway models for reaching the gas-exchange region in either a monopodial or a bipodial/tripodial airway branching system. From Crapo et al. (1990).

ter) in the trachea and larger TB airways caused by diffusion (Cohen, 1987; Cohen et al., 1990).

Alveolar Region Structure and Function

Because the alveolar region is where gas exchange occurs, a teleological argument often has been made that the types of cells in this region should be essentially the same in various mammalian species. The work of Stone and colleagues (1992) amply demonstrated that there is significant structural homogeneity of alveolar cells in mammals ranging over more than five orders of magnitude in body weight (i.e., from the shrew to the horse). The larger surface area of the human lung arises from more, not necessarily larger, cells than are in the alveolar region of the rat. Given the larger amount of tissue to support as the lung increases in size, there is a corresponding linear increase in both collagen- and elastin-rich fiber systems as the body weight of mammalian species increases (Mercer and Crapo, 1990). However, because collagen and elastin fibers are concentrated at alveolar entrance rings, Mercer and Crapo (1990) found that the normalized volume density of collagen and elastin fibers at these locations was 10-fold greater in humans compared to mice, despite the fact that an alveolus in a human lung is only four-fold larger than the alveolus in a mouse. The role these differences may play among species in fibrotic responses caused by prolonged exposure to relatively insoluble particles is unknown.

The liquid layer lining the alveolar epithelium is composed of surfactant, which contains a number of surface-active materials, primarily phospholipids. Surfactant lowers the work of breathing by lowering surface tensions, thereby stabilizing alveoli and preventing them from collapsing. The surfactant layer is nonuniform in that there is a thin film (<0.01 μm thick) on a hypophase approximately 10 times thicker, but there is significant pooling of surfactant in corners (pockets) of alveoli during expiration. The phospholipid composition of lung surfactant is remarkably similar between rats and humans (see Rooney, 1992, Table 7). Because airflow velocity reduces with each bifurcation of the airways, airflow in the alveolar region is low and is essentially laminar. Even at flow rates 10 to 15 times greater than needed for normal respiration, convection is only 12% as important as diffusion for gas transport (Davidson and Fitz-Gerald, 1974). As a result, diffusion is the primary mechanism by which particles smaller than 0.5 μm entrained in air that reaches the alveolar region are deposited. For particles larger than 1 μm d_{ae}, sedimentation is the dominant mechanism for alveolar region deposition.

The material presented thus far clearly demonstrates that complex interactions among species-specific respiratory tract anatomy, the route and depth of breathing, and particle-specific physical factors determine the sites of deposition of particles at various locations within the respiratory tract (Fig. 5). In addition, the relative importance of the major mechanisms by which deposition occurs is influenced by these factors. For both rats and humans, impaction predominates in the ET region, and diffusion largely governs deposition in the alveolar region. The relative impor-

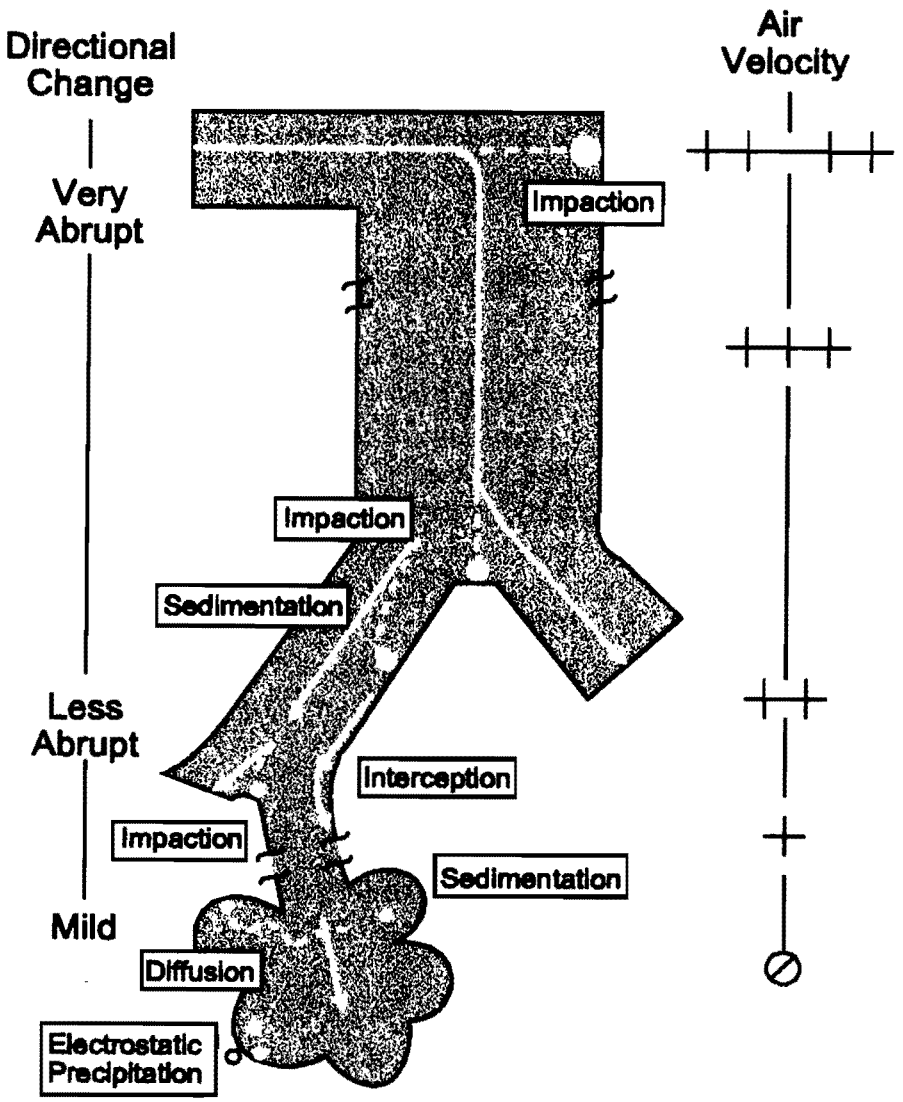

FIG. 5. Schematic representation of major mechanism governing the deposition of particles in the respiratory tract. Airflow is signified by the arrows and particle trajectories by the dashed lines. Modified from U.S. Environmental Protection Agency (1996).

tance of impaction and sedimentation vary significantly between rats and humans, primarily because of differences in airway size and overall lung architecture. Both processes are important for TB deposition in rats, but impaction is the predominant mechanism for TB deposition in humans.

EXPERIMENTAL DATA ON REGIONAL DEPOSITION

A number of experimental studies on the regional deposition of solid particles have been conducted using healthy, adult human subjects. Many fewer data are available from animal studies specifically designed to determine regional deposition of parti-

cles. For a detailed review of experimental deposition data for solid particles and for a discussion of the limited data available on the deposition of hygroscopic particles, the reader is referred to Chapter 10 of the U.S. Environmental Protection Agency's (1996) document on air quality criteria for particulate matter. Here, overall trends in deposition of solid particles are briefly reviewed.

ET Region Deposition

Recall that impaction is the predominant mechanism for deposition of particles in the ET region and that humans breathe through both the nose and the mouth, depending upon activity level or medical condition. Thus, an impaction parameter, $d^2_{ae}Q$, where Q is the inspiratory flow rate, is used to relate deposition efficiency when breathing through the nose (Fig. 6) as compared with the mouth (Fig. 7). Several conclusions are apparent from the data shown in Figures 6 and 7. (1) There is a tremendous increase in variability in deposition efficiency as values of the impaction parameter increase from 100 to 10,000 $\mu m^2\ cm^3\ s^{-1}$ for nasal breathing; (2) because the size of the ET region during mouth breathing increases with increasing flow rate and tidal volume, the empirical equation fit to the deposition efficiency

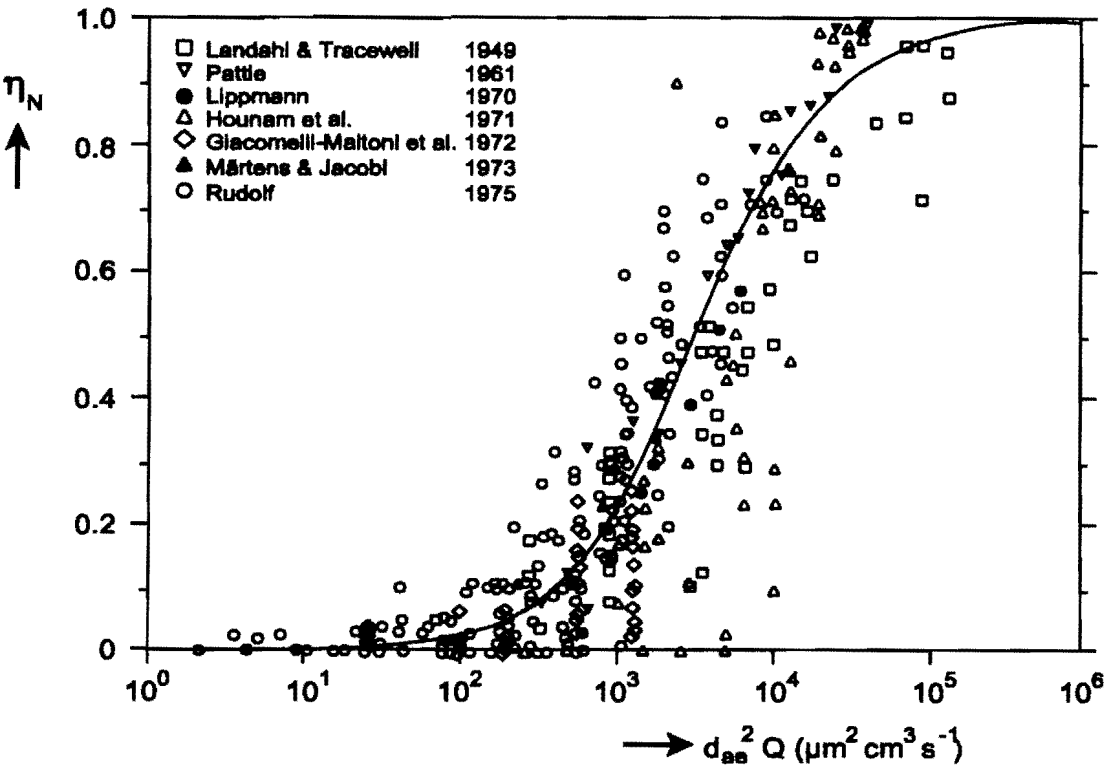

FIG. 6. Inspiratory deposition in the human nose as a function of particle aerodynamic diameter and flow rate (d_{ae}^2Q). The curve represents the equation $\eta_N = 1 - [3.0 \times 10^{-4}(d_{ae}^2Q) + 1]^{-1}$. Data are from Stahlhofen et al. (1989), and equation is from the International Commission on Radiological Protection (1994).

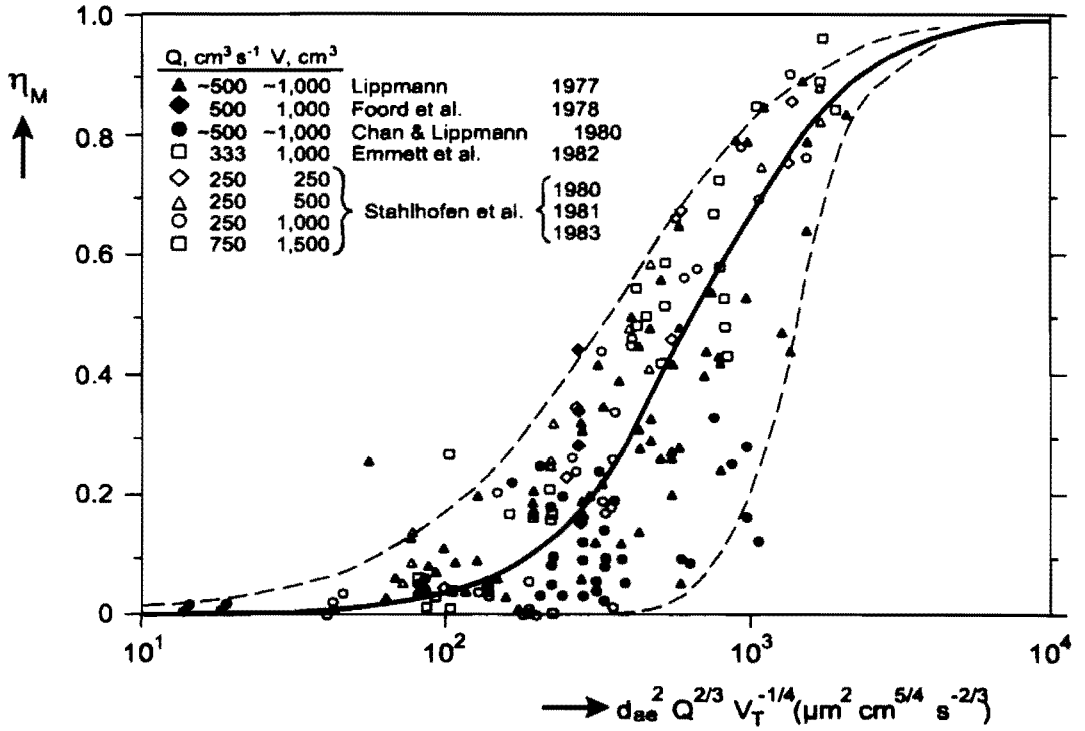

FIG. 7. Inspiratory extrathoracic deposition data in humans during mouth breathing as a function of particle aerodynamic diameter, flow rate, and tidal volume ($d_{ae}^2 Q^{2/3} V_T^{-1/4}$). The solid curve represents the equation $\eta_N = 1 - [1.1 \times 10^{-4} (d_{ae}^2 Q^{0.6} V_T^{-0.2})^{1.4} + 1]^{-1}$, with the dashed lines representing 95% confidence limits on the mean. Data are from Stahlhofen et al. (1989), and the equation is from the International Commission on Radiological Protection (1994).

data for mouth breathing is of a different form than that used for nasal breathing; (3) as with nasal breathing, there is significant scatter in the experimental data for ET deposition when inhaling through the mouth; and (4) nasal breathing is considerably more efficient in removing inhaled particles than is oral breathing.

Experimental data on the deposition of particles in the ET region of various laboratory animals are shown in Figure 8. Overall, there is less variability in ET deposition of particles in animals compared with humans.

TB Region Deposition

Particles that penetrate the ET region can be deposited in TB airways. Only an indirect assessment of deposition in this region is possible in human experimental studies. Because the experimental studies use radiolabeled particles, the amount of activity retained in the lung as a function of time is determined; then TB deposition is derived from the fast-decay component (i.e., the first 24 hours) of the activity curve, with alveolar deposition being estimated from the slow-decay portion of the activity curve. The rationale for this approach to determining TB and A deposition is that

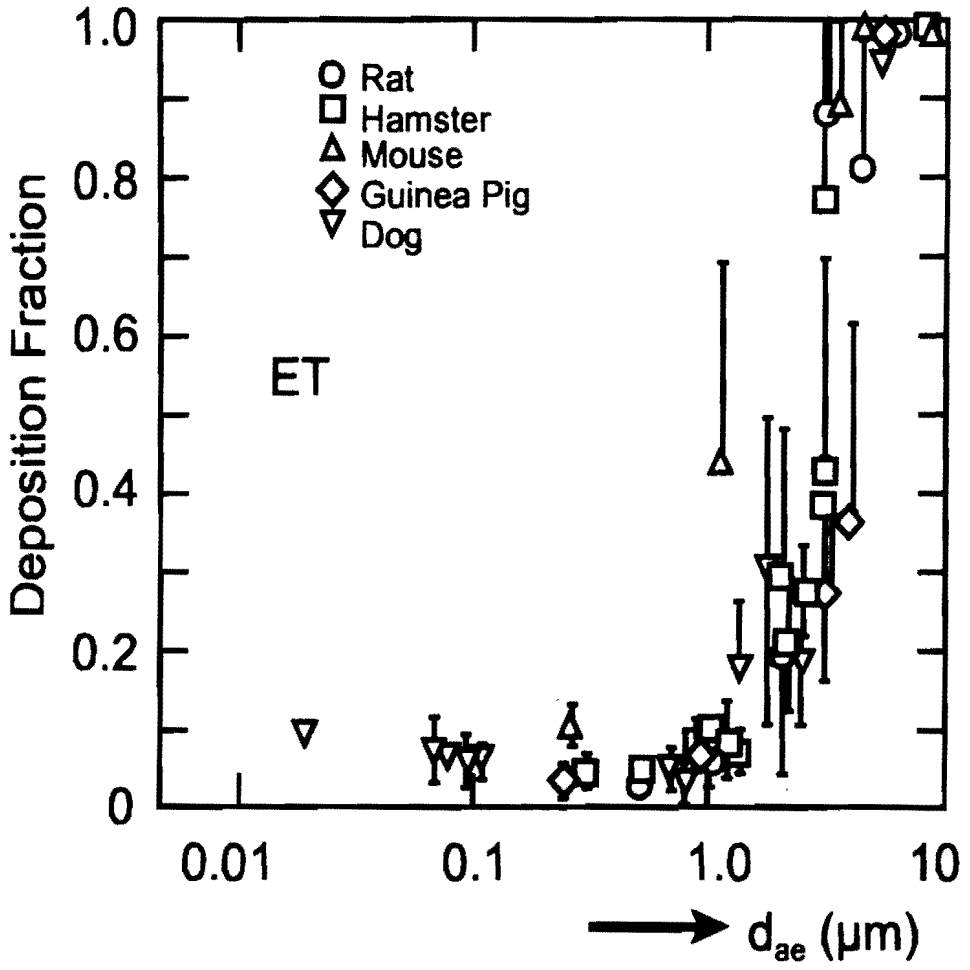

FIG. 8. Extrathoracic (ET) deposition fractions in various animal species as a function of particle aerodynamic diameter. For those smaller than 0.5 μm, geometric diameters were used. Data are from Schlesinger (1988), reprinted with permission, copyright by the National Academy of Sciences. Courtesy of the National Academy Press, Washington, DC.

the fast- and slow-decay components are considered to represent mucociliary and macrophage clearance, respectively. However, the cut point of 24 hours for TB airway deposition is somewhat arbitrary, as there is experimental evidence in support of the concept that some material deposited in the TB region is retained considerably longer than 24 hours (Scheuch and Stahlhofen, 1988). The factors responsible for this observation have not been elucidated, although phagocytosis by airway macrophages, an incomplete mucous layer, and flow mixing all have been postulated as potentially being involved. In addition, heterogeneity in TB path length to the alveolar region could be a factor. Whatever the reason, it is likely operative in rats as well as humans.

Experimental data for TB deposition of particles in humans are shown in Figure 9. Of note is that the data represent deposition fractions rather than deposition effi-

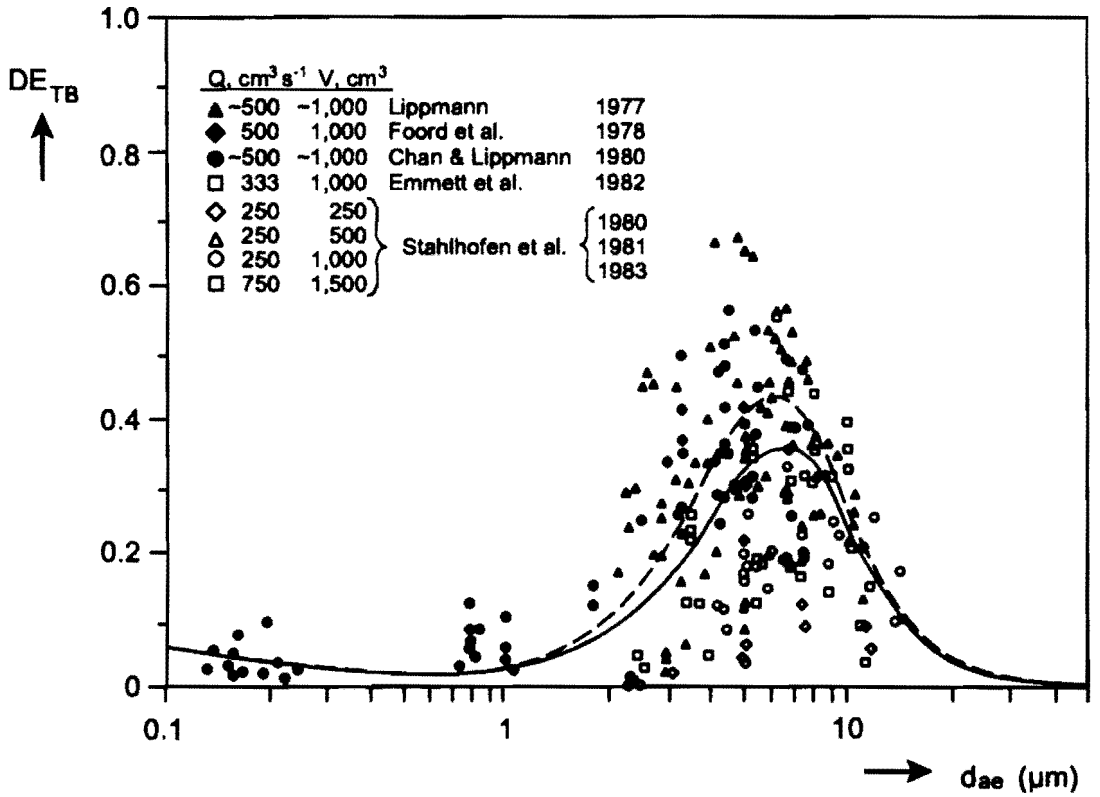

FIG. 9. Tracheobronchial deposition data in humans with mouth breathing as a function of particle aerodynamic diameter (d_{ae}). DE_{TB} represents the fraction of particles depositing in the tracheobronchial region out of the total inhaled. The *solid curve* represents the approximate mean of all the experimental data; the *broken curve* represents the mean excluding the data of Stahlhofen and colleagues. Data are from Stahlhofen et al. (1989).

ciencies. Although deposition fractions and efficiencies are the same for the ET region, the same cannot be said for the TB region. If the deposition data were expressed as the number of particles depositing in the TB region divided by the number of particles entering this region, the result would be TB deposition efficiencies that would asymptotically approach one as particle size increased. For a discussion of the relationship between deposition fractions and efficiencies and how they can be calculated for the ET, TB, and alveolar regions, the reader is referred to work by Ménache et al. (1996).

Considerable scatter can be seen in the TB deposition data in Figure 9. This scatter is caused by differences in experimental techniques, intra- and intersubject variability, and flow rates used in the various studies, coupled with the fact that d_{ae} is used on the abscissa. Because impaction is directly proportional and sedimentation is inversely proportional to flow rate, a single relationship between deposition and d_{ae} for different flow rates is not possible. Hence, combining data from experiments using different flow rates as was done in Figure 9 automatically imparts scatter. The peak deposition fraction in the TB region occurs for particles about 4 μm d_{ae}. Also, note that there is very modest deposition in the TB region for particles smaller than

1 μm d_{ae}. Regional respiratory-tract experimental data are not currently available for TB deposition in humans of ultrafine particles (i.e., particles with a physical diameter <0.1 μm). Dosimetry models predict deposition fractions to approach a peak of 0.6 for 0.005-μm particles and then to decrease as particle size decreases (International Commission on Radiological Protection, 1994). However, TB deposition studies of ultrafine particles in human replica cast (Cohen, 1987; Cohen et al., 1990) yield deposition efficiencies that are about two-fold higher than those predicted using dosimetry models.

Data on the fraction of particles deposited in the TB region of rats, hamsters, mice and other animal species are shown in Figure 10. TB deposition is minimal, being typically 5% to 10%, and is essentially uniform across these species for particles larger than 0.5 μm d_{ae}, at least within the error of measurement. Because there is nearly complete ET deposition of particles larger than 4 μm d_{ae} in rodents, TB deposition of such particles is correspondingly low.

Alveolar Region Deposition

Alveolar deposition fractions in healthy, adult humans as a function of d_{ae} are shown in Figure 11. As with other regional deposition data, significant scatter is de-

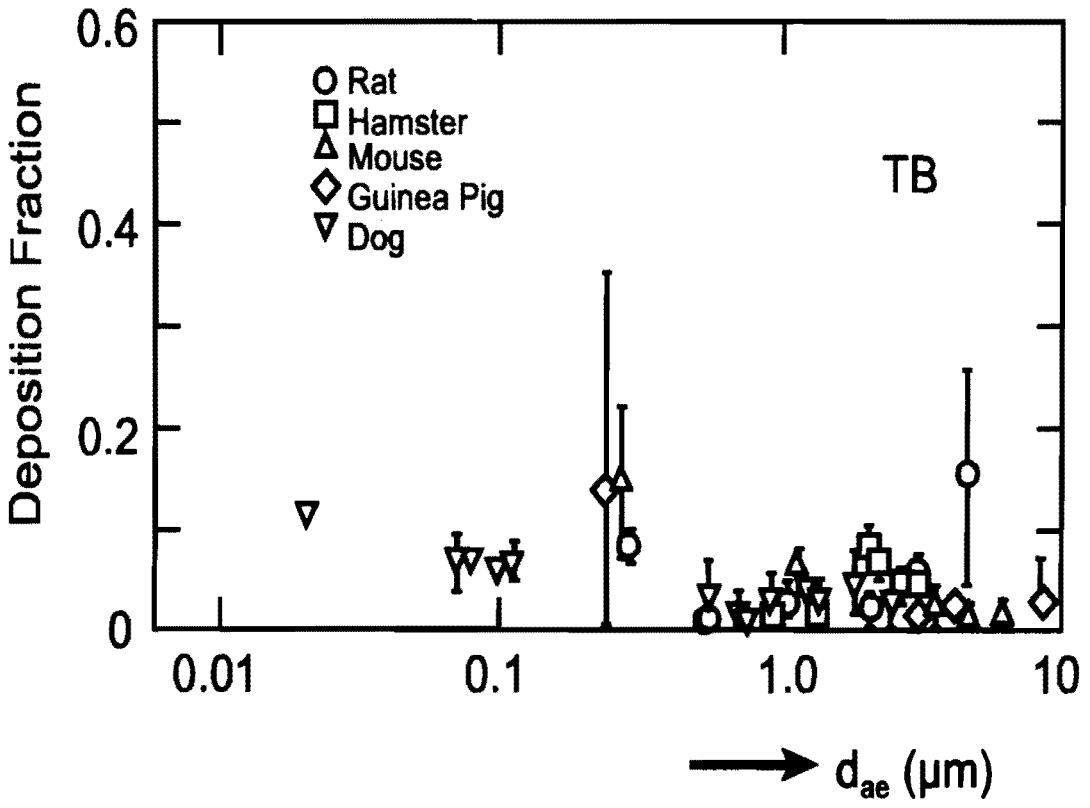

FIG. 10. Tracheobronchial deposition fractions in various animal species as a function of particle aerodynamic diameter; for less than 0.5 μm, geometric diameters were used.

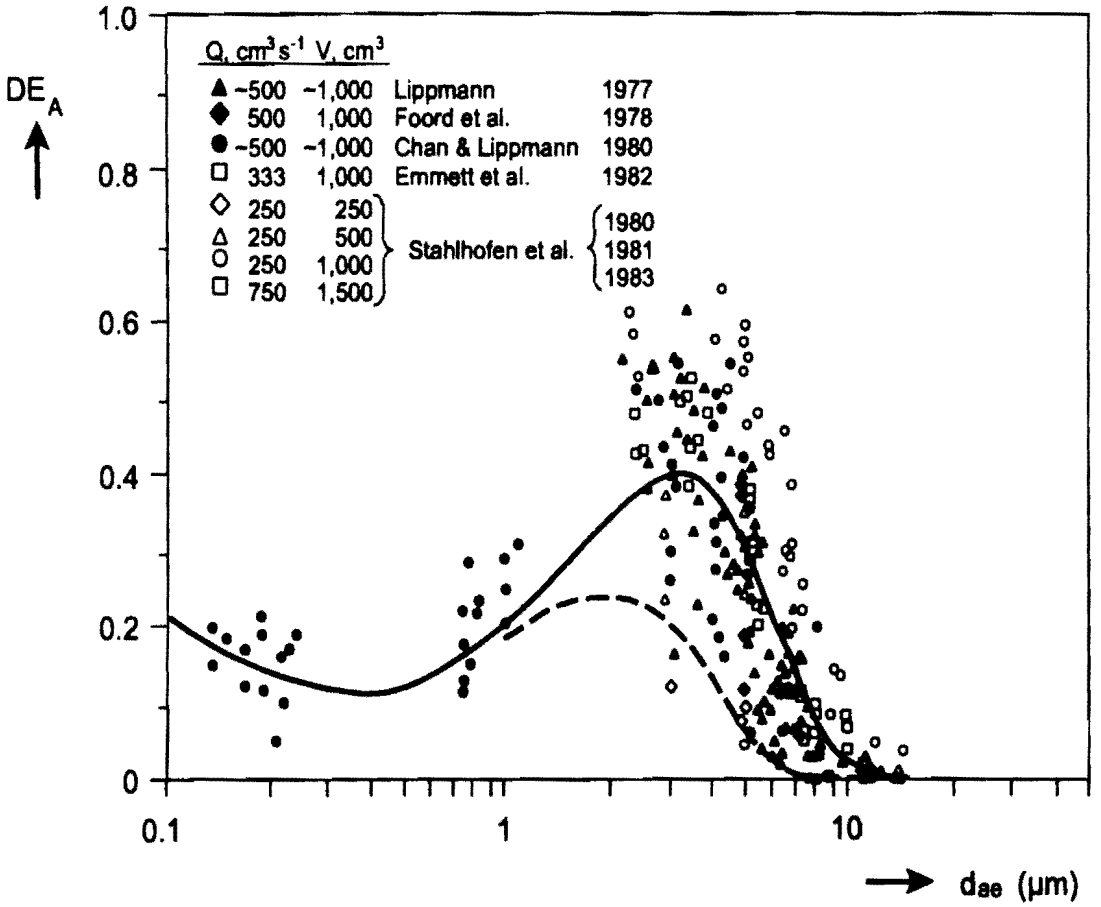

FIG. 11. Alveolar deposition data in humans as a function of particle aerodynamic diameter (d_{ae}). The *solid curve* represents the mean of all the data; the *broken curve* is an estimate of deposition for nose breathing by Lippmann (1977). Data are from Stahlhofen et al. (1989).

picted. For particles larger than 1 μm d_{ae}, there is enhanced alveolar deposition if individuals breathe through the mouth as compared with the nose, as indicated by the solid and dashed lines, respectively. Below 1 μm d_{ae}, the two routes of breathing yield similar alveolar deposition fractions. The peak for alveolar deposition occurs at a d_{ae} of about 3.5 μm.

Alveolar deposition in laboratory animals is depicted in Figure 12. In general, for most d_{ae}, alveolar deposition fractions in rodents are considerably lower than they are for humans. This observation often has been used by toxicologists to justify the use of exposure levels in animal inhalation studies of carcinogenicity that are many orders of magnitude greater than those likely to be encountered by humans. The use of such high exposures for PSP has led to the phenomenon of "lung overload" in carcinogenicity studies for such particles as carbon black, coal, diesel soot, talc, and titanium dioxide.

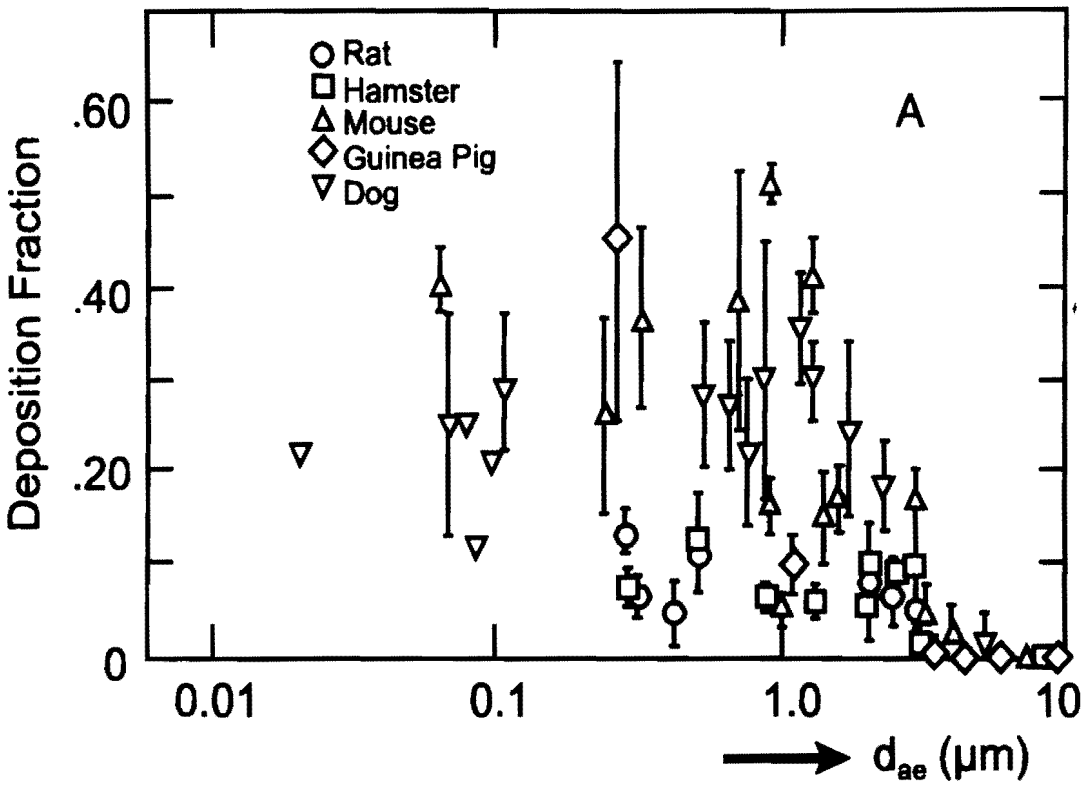

FIG. 12. Alveolar deposition in various animal species as a function of particle aerodynamic diameter (d_{ae}). For those smaller than 0.5 μm, geometric diameters were used. Data are from Schlesinger (1988), reprinted with permission, copyright by the National Academy of Sciences. Courtesy of the National Academy Press, Washington, DC.

SPECIES-SPECIFIC FACTORS INFLUENCING DOSIMETRY

Although species-specific structure of the various respiratory-tract regions in combination with the route and depth of breathing are critically important for determining where particles will deposit, there are several other factors that affect dosimetry to differing degrees in laboratory rodents and humans. Among these factors are inhalability, oronasal breathing, and heterogeneity in acinar deposition of particles. In addition, there may be morphometric differences in alveolar parameters that influence the choice of appropriate dose metrics for relating various types of effects. These topics are discussed briefly.

Inhalability

Laboratory animals and humans inhale particles from the air space proximal to the nares, and humans also may inhale particles from air proximal to the mouth. The air space around these orifices is considered to be the breathing zone. The penetration of particles into the breathing zone is influenced by airflow velocity and direction in

close proximity to a person's or animal's head and body. Inhalability can be defined as the probability that a particle of a given size actually will enter one of the respiratory-tract orifices in the case of humans or enter the nares in the case of laboratory rodents, because these animals are obligatory nose breathers. Using this probability, one can adjust the concentration of particles external to the human or animal to obtain the concentration of particles in the inspired air.

Because inhalability of particles varies among species (Ménache et al., 1995), adjustments for inhalability must be made when making interspecies comparisons of exposure scenarios that lead to the same internally deposited dose. Inhalability in humans is not a factor for particles studied thus far in animals, because the particle size range of the aerosols have not exceeded 5 μm d_{ae}, and because particles smaller than 5 μm d_{ae} are completely inhalable by humans.

Using the experimental data of Raabe et al. (1988), Ménache and colleagues (1995) determined that a logistic curve adequately described the probability that laboratory rodents would inhale particles of any given size. Even for particles as small as 1 μm d_{ae}, rats inhale only 93% of particles this size. Inhalability declines with increasing particle size such that 85%, 77%, 71%, and 65% of 2-, 3-, 4-, and 5-μm d_{ae} particles, respectively, are inhaled by laboratory rodents. Independent of any difference between rats and humans in the clearance of particles, suppose one wanted to know to what level humans would have to be exposed to get the same mass of particles per unit surface area deposited in the alveolar region if rats were exposed for 1 hour to 5 mg/m^3 of a monodisperse aerosol of 2-μm d_{ae} particles. Using fractional alveolar deposition data for humans and rats, the inhalability equation for rodents developed by Ménache et al. (1995), pulmonary function data specific to each species, and computational procedures described by Miller et al. (1995), one finds that humans exposed for 1 hour to 1.85 mg/m^3 of this aerosol would have the same mass deposited per unit surface area in the alveolar region as would rats. The computation is, of course, more complex for polydisperse aerosols.

Oronasal Breathing

As noted previously, laboratory rodents are obligatory nose breathers, but humans can breathe through either their nose or mouth. For most of the human population, individuals breathe through their nose while at rest. As ventilatory drive increases with work or exercise, humans switch to oronasal breathing when minute ventilation exceeds about 35 L/minute (Niinimaa et al., 1981). The proportion of inhaled air entering through the mouth continues to increase as minute ventilation increases beyond the oronasal switching point. Niinimaa and colleagues (1981) found, however, that 15% of subjects breathe through their mouth even at rest. Because oronasal breathing modifies the amount and the pattern of particle deposition, the activity pattern of the human subpopulation being exposed to particles of concern needs to be taken into account. Deposition equations and regional respiratory-tract deposition curves that incorporate oronasal breathing have been developed by Miller et al. (1988).

Heterogeneity in Acinar Deposition

Alveolar-region deposition of particles is typically of concern because clearance of particles from this region is slow. To date, experimental particulate studies for the most part have provided information only on particle deposition aggregated over large regions of the lung. The rat lung has over 2400 acini, and there is significant variability in TB path length to reach these acini (Yeh and Harkema, 1993). Anjilvel and Asgharian (1995) developed a multiple-path model for the TB region of the rat and used this model to determine particle deposition in each acinus of the lung as a function of particle size. They studied various particle sizes and found that heterogeneity among acini in particle deposition is greatest if particles are relatively small ($\leq$0.1 μm). Even for particles in the range of 1 to 3 μm d_{ae}, there is considerable variability in particle deposition among acini in the rat lung, with about 100 acini and 50 acini having deposition fractions about 25% and 50% greater, respectively, than the average.

MECHANISMS OF CLEARANCE AND TRANSLOCATION

Once particles have deposited on airway surfaces, they are cleared or translocated to other sites either within the respiratory tract or external to it. The mechanisms that are operative for clearance and translocation of particles differ among the ET, TB, and A regions. Table 3 provides a breakdown of where various clearance mechanisms are operative in the major respiratory tract regions. Most of the clearance mechanisms involve mechanical transport of intact particles, with dissolution of particles essentially being the only absorptive process. Information on the rate of dissolution of particles compared with their rate of clearance by mechanical transport is used to classify particles along the spectrum from highly soluble to poorly or insoluble. For particles exerting toxicity or carcinogenicity through the phenomenon of lung overload, the rate of clearance by dissolution is insignificant compared to the rate of clearance of the intact particles.

TABLE 3. *Importance of various clearance mechanisms in major regions of the respiratory tract*

Clearance mechanism	Extrathoracic region	Tracheobronchial region	Alveolar region
Nose wiping and blowing, sneezing	X		
Mucociliary transport	X	X	
Dissolution			
Soluble particles	X	X	X
Poorly soluble particles			X
Coughing		X	
Macrophage phagocytosis		X	X
Interstitial			X
Epithelial cells		X	X

Note: X indicates that the mechanism is a factor in the region in question.

The dissolution rate of solid particles depends upon one or more of the following: (1) the surface area of the particles exposed to the medium containing them, (2) the diffusion of molecules through the stagnant layer of media around the particles, and (3) diffusion to the surface of the more soluble components of multicomponent particles (Moss and Kanapilly, 1980). By their very nature, hygroscopic particles and liquid droplets dissolve instantly upon contact with the mucous layer in the ET and TB regions or with the surfactant layer in the A region. For a detailed discussion of dissolution kinetics, the reader is referred to work by Moss and Kanapilly (1980); for consideration of the role of particle size in the dissolution of body burdens arising from a log-normally distributed population of particles, the reader is referred to work by Mercer (1967).

ET Region Clearance

The most anterior portion of the nose contains nasal hairs that trap most of the large particles (> 10 μm) that are inhaled. Squamous cells make up the epithelium in this region, which is not lined with a layer of mucus. Thus, clearance of particles occurs only by wiping or blowing. For respiratory and transitional epithelium that lines posterior ET regions, complex flow patterns of mucus, which is propelled by the beating of ciliated cells, lead to solid particles moving towards the nasopharynx and eventually being swallowed. Poorly soluble particles deposited in oral passages are cleared by coughing, expectoration, or swallowing. Although some mucins may be seen overlying olfactory epithelium, there is not a continuous layer of mucus in this region; a combination of mucous and serous cells and ducts that transverse the olfactory epithelium provide the secretions for the surface of the olfactory epithelium (Getchell and Getchell, 1992). Once poorly soluble particles have deposited on olfactory epithelium, they can have extended periods of time for bioavailability. This may lead to uptake by olfactory cells and to retrograde neuronal transport such as has been demonstrated for cadmium (Hastings and Evans, 1991). Once deposited on ET epithelium, highly soluble particles likely are absorbed rapidly into epithelial cells.

TB Region Clearance

The primary mechanism for clearance of nonhygroscopic and relatively insoluble particles from the TB region is via the mucociliary escalator. The mucous layer lining the conducting airways is continually propelled cephalad by the beating of cilia until reaching the oropharynx, where the fluid is swallowed. In large airways, deposited particles tend to move in a spiral fashion on the mucous layer from the site of initial deposition until reaching the dorsal surface, after which they proceed longitudinally along this surface to the larynx (Wolff and Muggenburg, 1979). The nature of particle movement on the mucociliary escalator has not been examined in small airways. As noted earlier, the thickness of the mucous layer varies by location. Although some investigators have reported that the mucous layer is not contin-

uous, others have reported it to be continuous (Table 2). Regardless, there is general agreement that some regions within airway bifurcations have areas of nonciliated cells, leading to retarded clearance of particles from these areas. Interestingly, airway bifurcations have been shown to be hot spots for particle deposition resulting from enhanced impaction losses at these sites during inspiration.

Clearance of particles from the trachea and large TB airways can be facilitated in humans by coughing. Although a minor mechanism for clearance in healthy subjects, cough can be very important in individuals with severe respiratory disease, in which coughing serves to dislodge mucus and other deposited material from the surfaces of larger airways. Another potential mechanism for TB clearance of particles is through phagocytosis by macrophages resident in the conducting airways. Gehr and colleagues (1990) have shown that particles initially deposited in conducting airways can be found retained in the airways in close association with the epithelium, and that such particles are coated with an osmiophilic film attributable to surfactant. Particles retained in close proximity to the epithelium would tend to remain there until engulfed by resident macrophages.

Alveolar Region Clearance

As can be seen from Figure 13, there are a number of mechanisms and pathways that can be important for the clearance or translocation of particles from the alveolar region. Which mechanisms and pathways are operative at any point in time is a complex function of exposure rate and level, particle size, particle number, and cur-

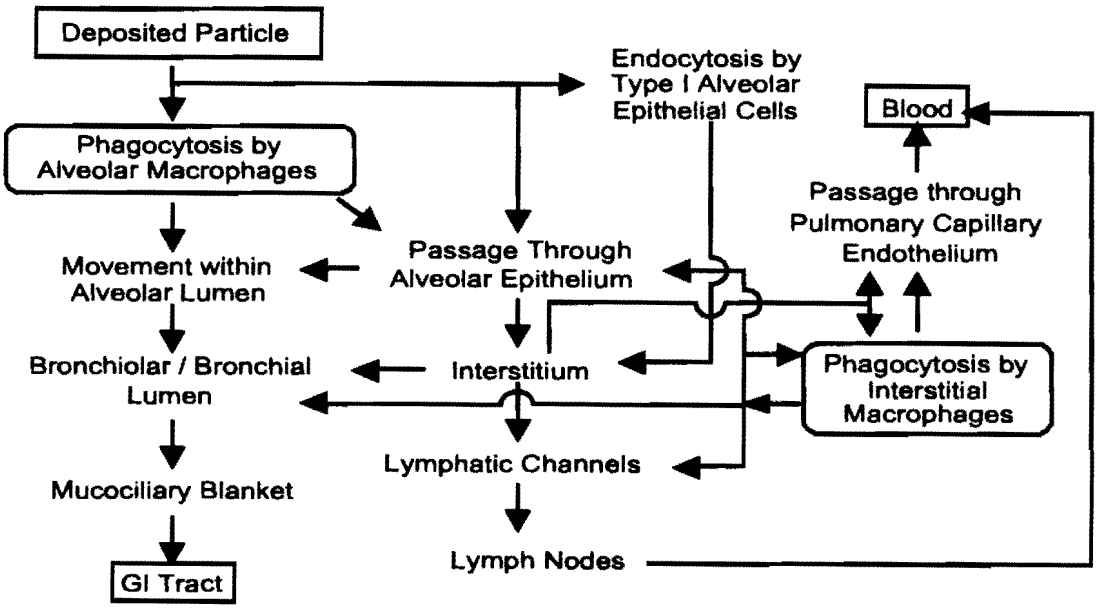

FIG. 13. Schematic of known and suspected clearance pathways for poorly soluble particles depositing in the alveolar region. Modified from U. S. Environmental Protection Agency (1996).

rent mass load. The same pathways for clearance of particles appear to be operative in laboratory animals and humans, although the relative importance of the various pathways appears to vary considerably among species (Snipes, 1989).

Alveolar macrophage phagocytosis of deposited particles is clearly the predominant clearance process for the alveolar region. Macrophages reside on the epithelium and come into contact with particles through either random motion or through chemotactic factors (Warheit et al., 1988). Chemotaxis may not be requisite for phagocystosis of particles by macrophages—Hadley (1977) calculated that a single rat AM can scavage approximately 35% of an alveolus of this species using "agrapod-like" extensions of its cell membrane. Despite tremendous differences in lung size, number of alveoli, and number of AMs between laboratory rodents and humans, the amount of epithelial surface area per AM is amazingly similar across these species (Table 4).

Translocation from the alveolar region of particles that have been ingested by macrophages primarily occurs by one of two pathways: (1) the mucociliary escalator or (2) pathways to the lung-associated lymph nodes. As can be seen in Figure 13, the pathways leading to particles ending up in such nodes are relatively torturous compared with translocation of particles via the mucociliary escalator.

Some of the particles passing through the alveolar epithelium and into the interstitium escape phagocytosis by interstitial macrophages. These particles contribute to the interstitial load and can move to various sites (perivenous, peribronchiolar, lymphatics, subpleural) before becoming trapped and increasing lung particle burdens. Accumulation of particles in interstitial spaces with chronic exposure to high levels of poorly soluble particles is a hallmark of the lung-overload phenomenon (Morrow, 1994). Uningested particles in the interstitium also may pass through the capillary endothelium and directly enter the blood stream (Raabe, 1982).

TABLE 4. *Interspecies comparisons of number of alveoli and of alveolar macrophage (AM) morphometric data*

	No. alveoli	No. AM	No. AM/ alveolus	Epithelial surface area per AM (μm^2)	AM volume (μm^3)
Mouse	4.2×10^6	2.9×10^6	0.7	17,200	493
Hamster	6.9×10^6	10.5×10^6	1.5	20,400	534
F344 rat	18.4×10^6	29.1×10^6	1.6	14,100	882
Sprague–Dawley rat	19.7×10^6	26.9×10^6	1.4	14,900	1161
Human	486×10^6	$5{,}990 \times 10^6$	12.3	17,100	1474

Note: Data for number of alveoli are from Mercer, Russell, and Crapo (1994) or derived from allometric relationships given by these authors. All other data are taken or derived from data in Stone et al. (1992) except AM volume for F344 rat, which is the average of values reported by Barry et al. (1985), Chang et al. (1986), Stone et al. (1992), and Mercer et al. (1995), and the AM volume for the Sprague–Dawley rat, which is the average of values reported by Crapo et al. (1978) and Stone et al. (1992).

CLEARANCE KINETICS

The potential for inhaled particles to exert toxic or carcinogenic effects is greatly influenced by their residence time at target sites. Residence time is particularly important for rodent inhalation studies using PSP, because particle–tissue contact is not diminished much by dissolution of the particles during the short life span of rodents. Clearance kinetics are influenced by a number of factors such as the inhaled particle size distribution, the respiratory pattern used, and the respiratory-tract anatomy of the species being studied (Wolff, 1992). As a result, there are significant differences among species in rates of clearance of inhaled particles from the ET, TB, and A regions. The net result of these species and regional differences presents a clear challenge to toxicologists and risk assessors for interpreting results from animal studies as to their relevance to humans.

ET Region Clearance Kinetics

Mucous flow rates are highly variable in different portions of the ET region both within and among species (see Table 2). The median mucous flow rate in healthy adults has been estimated to be about 5 mm/minute, thereby requiring a transport time of only 10 to 20 minutes for solid particles to travel from the anterior to posterior portions of the nasal passages (Rutland and Cole, 1981; Stanley et al., 1985). Because particles deposited on the more anterior portion of the nasal epithelium clear at a rate of only 0.017 to 0.033 mm/minute (Hilding, 1963), sneezing, wiping, or nose blowing typically is needed to remove such particles in a reasonable time frame. Although there is a paucity of olfactory epithelium clearance kinetic data, olfactory clearance is likely relatively slow compared with clearance from other ET regions.

TB Region Clearance Kinetics

Clearance of solid particles from ET areas lined with mucus is typically less than 30 minutes. Although the rich vascularization of the nasal region aids in humidification and thermal regulation of inspired air, the rapid dissolution of highly soluble and hygroscopic particles leads to absorption into the blood as a significant clearance mechanisms for such material.

Mucous velocities and hence the transport of particles vary considerably (Table 2) in different-sized TB airways. This variability is over and above the variability imparted by the use of various experimental methods to assess clearance rates in laboratory animals and humans (Schlesinger, 1985). Interindividual variability can be largely overcome by the use of radiolabeled particles and repeated measurements on the same subject or animal, because highly reproducible results are usually obtained for any given subject or animal. For the percentage of particles depositing in the TB region, 90% of relatively insoluble particles are cleared within

2.5 to 20 hours (Albert et al., 1973), and bronchial clearance is about 99% complete by 48 hours after exposure (Bailey et al., 1985). Individual subjects' geometry of the conducting airways and particle size are important sources of variability in measurements of TB clearance rates.

Some aspects of TB clearance remain controversial. Among these are conflicting interpretations concerning the reason why a small fraction (about 1%) of deposited particles appears to be retained for a long time (Gore and Patrick, 1982), compared with other investigations finding that up to 40% of particles likely to have been deposited in conducting airways are not cleared for days, and that this effect is inversely related to particle size (Stahlhofen et al., 1986). A surfactant film on the mucous layer, enhanced deposition at bifurcations and correspondingly low clearance from these areas, as well as heterogeneity in TB path length and the presence of airway macrophages, have been postulated as potential explanations.

Alveolar Region Clearance Kinetics

In general, clearance of particles from the alveolar region consists of two phases. The first phase is typically measured in days; the slower second phase occurs over a period of months to years. In addition to variability imparted by the use of different techniques, the physicochemical properties of the particle are important determinants of alveolar region clearance kinetics. A particularly important observation for particles for which lung overload has been shown to be operative is the fact that once any dissolution has been accounted for, mechanical removal by AMs via the mucociliary escalator or the lymphatics appears to be independent of size for particles smaller than 5 μm d_{ae} (Snipes et al., 1983). This finding justifies the synthesis of results from a wide variety of particle types and sizes in considering lung-overload issues. Given the wide range of clearance rates of identical particles among human subjects (Bailey et al., 1985), however, chronic exposures are associated with large variations in alveolar region particle burdens, thereby leading to significant uncertainties about comparable exposure scenarios between laboratory rodents and humans. In addition, because rats have more rapid alveolar clearance kinetics than do humans (Snipes, 1989), the difficulty in identifying equivalent exposure scenarios in these two species is compounded but approachable through the use of dosimetry models.

Although overall alveolar region clearance kinetics have been studied, data on clearance kinetics along the various clearance pathways depicted in Figure 13 are scant. Uningested particles can penetrate into the interstitium via endocytosis of type 1 epithelial cells in a matter of hours following deposition (Brody et al., 1981). This pathway has been shown to be increasingly important, as particle loading increases and appears to be even more important if particle levels exceed the saturation point for increasing macrophage number (Adamson and Bowden, 1978).

Clearance kinetics via the lymphatic system appear to be temporally dependent upon effectiveness (or lack thereof) of other clearance pathways. Greenspan and

colleagues (1988) showed that, if the phagocytic activity of macrophages decreases, lymphatic translocation tends to increase. Lymphatic translocation rates appear to be particle size–dependent in rats for particles in the aerodynamic size range, with smaller particles translocating faster than larger ones (Snipes and Clem, 1981; Takahashi et al., 1992). Although comparable data are lacking for humans, similar relationships likely hold also in people. Translocation rates to the lymphatic system are on the order of 0.02% to 0.003% per day (Snipes, 1989), with elimination from the lymph nodes occurring over half-times likely to be in the tens of years (Roy, 1989).

DOSIMETRY MODELS

In order to extend the results of an experimental dosimetry study to situations beyond the specific conditions of the given study, mathematical models incorporating deposition or clearance processes have been developed. An in-depth treatment of particulate dosimetry models is beyond the scope of this review; however, a brief discussion of the types of deposition and clearance models that are available is provided, together with citations to which the reader can refer (e.g., U.S. Environmental Protection Agency, 1996; Stöber et al., 1993, Schlesinger, 1989) for more complete treatments on deposition and clearance models for inhaled particulate matter.

Deposition Models

A variety of modeling approaches has been used to examine the deposition of particles in the respiratory tract. These approaches break down into two major categories. One category involves models incorporating a representation of airway structure in which equations for deposition efficiencies are solved by some computational algorithm that also accounts for the transport of particles through the airways. The other category involves empirical modeling of experimental data on deposition and clearance, typically using as parameters expressions involving airflow and particle characteristics (Rudolf et al., 1983, 1986, 1990). The most widely used empirically based model for the deposition of particles in the ET, TB, and A regions in the respiratory tract of humans is the latest effort by the International Commission on Radiological Protection (1994). The reader is referred to a publication by the U.S. Environmental Protection Agency (1996) for an overview of how the regional deposition values obtained using the International Commission on Radiological Protection model compare with the available body of experimental data in humans.

To date, the most widely used nonempirical dosimetry models for particle deposition in humans have been based largely upon typical path, whole-lung geometry models (Gerrity et al., 1979; Yeh and Schum, 1980; Yu and Diu, 1983; Egan and Nixon, 1989; International Commission on Radiological Protection, 1994). Such is also the case as for rats (Schum and Yeh, 1980; Xu and Yu, 1987; Martonen et al.,

1992). Typical path models often are referred to as *trumpet models* because the cumulative cross-sectional area gradually increases as one proceeds distally from the trachea through the conducting airways and then rapidly expands because of the tremendous increase in surface area in the alveolar region

As the computational speed and memory of computers increase, models for the lower respiratory tract deposition of particles can be developed that represent a refinement of typical-path, whole-lung models. Lobar-specific anatomical data for rats (Yeh et al., 1979) and for humans (Yeh and Schum, 1980) allow deposition models to estimate particle deposition on a lobar basis. This feature allows for better comparison of theory and experimental deposition data in rat inhalation studies, because often only a single lobe in the rat lung is used to determine body burdens. Lobar-specific deposition estimates in humans offer the potential to better understand deposition in diseased lungs because, as is the case for individuals with chronic obstructive pulmonary disease, there can be significant heterogeneity in lobar ventilation (Bates et al., 1971; Bates, 1989).

Beyond the typical-path, whole-lung, and lobar-specific anatomical structures, the detailed lung cast measurements made by Raabe and coworkers (1976) have been used in deposition modeling in two relatively complex ways. Anjilvel and Asgharian (1995) developed a multiple-path model for the rat lung in which they solved for particle deposition in each of the 2404 unique conducting airway paths and in the symmetric acinar structure they attached to the end of each path. An airflow splitting algorithm was used that invoked the assumption that flow partitioning is proportional to distal volume. These investigators also have used their asymmetric, multiple-path model to study fiber deposition in the rat lung (Asgharian and Anjilvel, 1998). The other way the data of Raabe et al. (1976) have been used is in stochastic models of lung deposition that employ Monte Carlo methods and that exploit the statistical distributions of the morphometric data (diameters, lengths, branching, and gravity angles) for individual airway generations as well as correlations between daughter and parent airways and major to minor daughter airways. Hofmann, Koblinger, and colleagues have been leaders in the development and use of stochastic lung modeling to study various aspects of the deposition of particles in the human lung (Koblinger and Hofmann, 1985, 1988, 1990; Hofmann and Koblinger, 1990, 1992), in the rat lung (Koblinger and Hofmann, 1995; Koblinger et al., 1995), and in comparisons between these two species (Hofmann et al., 1989; Hofmann and Koblinger, 1994; Hofmann and Bergmann, 1998; Hofmann et al., 1999).

As opposed to the extensive use of computational fluid dynamic models for the upper respiratory tract, there are currently no published data on the use of such modeling in the lung. In the future, one can envision the use of these models to examine deposition "hot spots" such as at airway bifurcations or to study gas–particle interactions in selected areas of the lung. However, computational fluid dynamic models of the entire lower respiratory tract present a computational nightmare for the study of particle deposition. Indeed, the supercomputer computational intensity needed for the algorithm developed by Martonen et al. (1994) to interpret planar gamma camera images obtained in conjunction with aerosol therapy has severely

restricted the use of this technique. More recently, Martonen and colleagues (1997) incorporated a method to map the three-dimensional outer boundary of the lung based on Delaunay tessellation (Martonen et al., 1994) and other more clinician-friendly features to develop a newer algorithm that can run on workstations more likely to be available at medical facilities. Dosimetry modelers need to be mindful of the biological or toxicological problem at hand so that dose resolution is at the appropriate level of detail.

Once a lung geometry has been selected and an algorithm developed to account properly for airflow resulting from the route and depth of breathing, equations for the various mechanisms by which particles are removed from the air stream must be solved to determine particle deposition. For solid, spherical particles, equations for impaction, sedimentation, and diffusion are given by Anjilvel and Asgharian (1995). In the case of fibers, the equations for some of the deposition mechanisms take on a different form (see Asgharian and Anjilvel, 1998). The diameter of hygroscopic particles changes as a function of the relative humidity to which the particles are subjected (Tang and Munkelwitz, 1977). Because temperature and relative humidity can vary among respiratory-tract locations, hygroscopic particles can either grow or shrink in size as they traverse respiratory-tract airways. For equations that can be used to examine the influence of impaction, sedimentation, and diffusion in the deposition of hygroscopic particles, the reader is referred elsewhere (Martonen, 1982; Martonen et al., 1985). Recently, Finlay (1998) described how two nondimensional parameters could be used to determine if (1) hygroscopic growth is significant but can be examined using a classical one-way coupled approach, (2) hygroscopic changes are not negligible but a two-way coupled approach can be used to study their behavior, or (3) hygroscopic growth changes are negligible.

Clearance Models

As evidenced from the material presented previously on clearance and translocation of particles and on the rates at which such events occur, the development of accurate models for the clearance of particles is a complex and difficult endeavor. The amount of deposited particles retained at specific respiratory tract sites continues to increase until the rate of deposition to the area is offset by the rate of clearance. As opposed to our knowledge and use of laws of physics that have enabled significant progress to be made in understanding the deposition of particles in animals and humans, our knowledge of how biological systems handle material once it has been deposited is much more rudimentary. The deposited material can interact with the biological environment of the respiratory tract in a number of ways, thereby giving rise to the various clearance mechanisms listed in Table 3.

Models for the clearance of particles can be broadly classified as either empirically or biologically based. Because biological systems are inherently variable, most clearance models that have been developed to date rely heavily on empirical relationships between variables known to be important in certain clearance path-

ways and experimental data on retained respiratory-tract burdens or other measurements relevant to the variables being examined. In the second edition of this book, Stöber et al. (1993) provided an extensive review of how the use of empirically based models of particulate clearance and retention in the lungs has developed since the 1950s. Since that review, the International Commission on Radiological Protection (1994) and the National Council for Radiological Protection (1997) have developed improved empirically based clearance models. Each of these groups divided the respiratory tract into more compartments than they had previously done, and they implemented empirical equations based upon more recent data in the literature. Although these models were developed for the radiological community, they can be used to examine the deposition and clearance of biopersistent particles in general. However, as noted by Stöber and McClellan (1997) for the International Commission on Radiological Protection model (and such would also hold for the National Council model), the nature of the additional compartments that were added reflect a way of approximating nonlinear processes, and, thus, these models do not apply for chronic exposures to high particulate burdens such as would be the case in lung overload.

Relative to the clearance of fibrous particulates, Yu et al. (1998) recently developed a semiempirical model for the clearance of man-made vitreous fibers from the lungs of rats. Major features of the model included accounting for (1) differential clearance of fibers by alveolar macrophages, (2) the dissolution rate of fibers in the pulmonary extracellular fluid, and (3) the breakage of long fibers into shorter components as a function of their in vitro dissolution rate. Currently, experimental data are lacking to develop a comparable model for the clearance of fibers from the human lung.

Although significant efforts have been expended developing biologically based models for vapors and gases (see Chapters 17 and 19), not until the phenomenon of lung overload had been identified were biologically based particulate clearance models proposed to account for the functional and biological structure of the alveolar region of the lung (Stöber et al., 1993). As Figure 13 conveys, there are a number of potential pathways for clearance of particles that have been deposited in the alveolar region. Developing a physiologically based model that incorporates the various pathways and kinetics relevant to them is indeed a formidable task. As in any field of modeling, simplifications often must be introduced either to make the problem mathematically tractable or to make use of the available biological data. In the 1980s, efforts to develop physiologically based models were made by various investigators (Soderholm, 1981; Strom et al., 1988; Smith, 1985; Stöber et al., 1989).

Stöber and colleagues (1989, 1990a,b, 1994) have been leaders in developing physiologically based clearance models for biopersistent particles of low toxicity. Katsnelson and coworkers (1992,1994) and Tran and colleagues (1994, 1995) have led efforts to develop physiologically based clearance models for biopersistent particles having inherent cytotoxicity. The initial biologically based models for all three of these groups can be viewed as "parameter rich and experimental data poor." Thus far, only Stöber and colleagues (1994) have extended their analyses to develop a simpler model version that is more commensurate with the amount of available biological

data. Some parameters in the model version, termed by Stöber et al. (1994) as "standardized design," take on fixed values; other parameters are material-specific and must be estimated for a given type of particle (diesel soot, carbon black, titanium dioxide, etc.) A wide variety of particle sizes, exposure concentrations, and duration of exposures has been studied. The standardized model predicts retention burdens that are in reasonable agreement with the experimental data, particularly for the longer-term exposure studies. For an in-depth review of recent progress in using physiologically based dosimetry models to examine the retention and clearance of poorly soluble particles of low toxicity, the reader is referred to Stöber and McClellan (1997).

LUNG OVERLOAD

Since Morrow (1988) reviewed the evidence for dust overloading of the lungs and postulated that the phenomenon reflected a breakdown of AM-mediated clearance of PSPs induced by a volumetric overload, additional experimental studies and insights about lung overload have led to a better characterization of general aspects of pulmonary responses during overload. These aspects include (1) stasis or slowing of AM-mediated clearance of PSPs, (2) significant and diverse accumulation of PSP-laden AMs within pulmonary alveoli, (3) increased translocation and accumulation of PSPs in the interstitium of the lung and in the lymph nodes of the thoracic cavity, (4) chronic inflammation in the lung, (5) the eventual appearance of alveolitis and granulomatous lung disease, and (6) the potential development of lung tumors (Snipes, 1995). Interestingly, despite evidence that studies using mice and hamsters have achieved lung burdens that are considered to be in the overload range, only rats have developed lung tumors, with no study of PSPs having identified lung tumors at a nonoverload exposure level. This has led to the question of the relevance of PSP-associated lung tumors for assessing potential carcinogenic risk to humans.

Although one of the hallmarks of lung overload is stasis or significant slowing of AM-mediated clearance of PSPs, there is not necessarily a decrease in phagocytic activity of AMs (Morrow, 1992). In fact, Morrow's (1992) analysis of the results of the particle clearance studies of Bellmann et al. (1991) led him to conclude that phagocytosis is a fast process relative to clearance and that phagocytosis by immobilized macrophages must continue to occur. Earlier, Morrow (1988) had hypothesized that volumetric loading of AMs was the driving function leading to the loss of mobility of these cells, with a threshold for the start of overload being 6% of the volume of an AM and with stasis occurring at a 60% volumetric loading level.

With a more definitive and broader array of lung morphometric data now available for laboratory rodents and humans (Stone et al., 1992), some interesting comparisons among species become apparent relative to the potential for volumetric loading of particles by AMs of various species (Table 5). After accounting for the volume of the AM nucleus and the void space volume (Stöber, 1972), one sees that only about 90 to 120 uniform, 1.9-μm particles would need to be engulfed to ex-

ceed the volume for stasis in rats rather than the about 150 such particles that Morrow (1988) computed. Such substantially lower numbers, as found in Table 5, for volumetric particle overload support the recent modeling work of Stöber et al. (1998) indicating that the initiation of lung overload may occur at considerably lower exposure levels than previously believed required (i.e., in the range of 150–200 $\mu g/ m^3$). Currently, however, there are no experimental data that can be used to confirm or refute these modeling predictions. Table 5 shows that essentially phagocytosis of a single 10-μm particle is sufficient to induce stasis of AMs in rodents and in humans. Interestingly, Oberdörster et al. (1992) showed that F344 rats can engulf such particles but do not appreciably transport them from the lungs.

Although the data in Table 5 give one some idea about the number of engulfed particles leading to stasis in various rodent and human AMs as a function of particle size, the time scale over which stasis might occur depends upon species ventilatory patterns and alveolar region morphometric parameters, the level and duration of exposure, and the rates of deposition and clearance of particles. If one ignores clearance, dosimetry calculations are available from Miller et al. (1995) that can be used together with the data of Table 5 to predict the earliest times at which stasis might occur for various exposure scenarios. Suppose, for example, that F344 rats and humans were exposed 24 hours per day to 10 mg/m^3 of aerosols of 1-μm or 5-μm particles. For 1-μm particles, about 80 days of exposure would yield stasis of AMs in rats compared with about 310 days in humans, and for 5-μm particles, the corresponding numbers would be 300 and 90 days, respectively. The fact that lung overload has been observed much later than these times in rodents exposed chronically to 10 mg/m^3 of PSPs reflects the importance of clearance as a mechanism to reduce the lung burden of particles.

Heterogeneity in acinar deposition in the rat lung, as noted earlier, means there is greatly enhanced deposition in some localized areas of the pulmonary region; this, coupled with the fact that rat AMs have anywhere from 65% to 135% greater volume than AMs from mice or hamsters (Table 4), may provide some insights about the lung overload phenomenon. Lung overload involves an inhibition or stasis of AM-mediated clearance of particles. If mouse, hamster, and rat AMs do not differ in the rate at which they can phagocytize particles, then achieving an ingested particle volume of 60% of the cell's volume, which Morrow (1988) postulated as leading to macrophage stasis, would require a longer period of exposure in rats than in mice or hamsters given comparable deposition efficiencies among these species. Eventual macrophage death in the rat would lead to a greater lung burden of particles than in the mouse or hamster, thereby leading to a greater influx of macrophages and an increased likelihood of a cascade of inflammatory processes. In addition, the ability of particles to accumulate in the interstitium would be greater in rats compared to mice or hamsters. All of this suggests that a wide variety of dose metrics as well as biological factors may need to be examined in order to understand the basis for species differences that may be involved in lung overload. To that end, Table 6 presents human-to-rat ratios for various dose metrics as a function of particle size.

TABLE 5. *Alveolar macrophage morphometric data in relationship to volumetric particle overload*

	Volume		Volume for cell stasis[c] (μm³)	Number of engulfed particles leading to stasis[d]										
	Cell[a] (μm³)	Nucleus[b] (μm³)		0.1 μm	0.5 μm	1 μm	1.5 μm	2 μm	2.5 μm	3 μm	3.5 μm	4 μm	5 μm	10 μm
Mouse	493	124	221	304,423	2,435	304	90	38	19	11	7	5	2	0.30
Hamster	534	117	250	344,022	2,752	344	102	43	22	13	8	5	3	0.34
F344 rat	882	121	456	627,407	5,019	627	186	78	40	23	15	10	5	0.63
Sprague–Dawley rat	1,161	153	605	831,181	6,649	831	246	104	53	31	19	13	7	0.83
Human	1,474	121	812	1,116,216	8,930	1,116	331	140	71	41	26	17	9	1.12

[a]Data for the mouse, hamster, and human are from Stone et al. (1992). Value for the F344 rat is average of Stone et al. (1992), Barry et al. (1985), Chang et al. (1986), and Mercer et al. (1995). Value for the Sprague–Dawley rat is average of Stone et al. (1992) and Crapo et al. (1978).

[b]Data are from Table 4 in Stone et al. (1992). The mean value of 121 μm³ was assigned to F344 rats and humans since Stone et al. did not give values for these species.

[c]Volume taking into account the volume of the cell's nucleus.

[d]Includes adjusting for the void space volume (Stöber, 1972) created by the packing of uniform spheres.

TABLE 6. *Human-to-rat ratios for various alveolar region dose metrics*

Diameter (μm)	Mass		Number of particles			
	Total	Per unit area	Per unit area	Per ventilatory unit	Per alveolus	Per macrophage
0.2	53	0.14	0.14	3.88	2.15	0.27
0.4	62	0.17	0.16	4.56	2.52	0.32
0.6	72	0.19	0.19	5.30	2.93	0.37
0.8	82	0.22	0.21	6.06	3.35	0.42
1	92	0.25	0.23	6.77	3.74	0.47
2	137	0.37	0.31	10.05	5.55	0.69
3	223	0.60	0.47	16.37	9.05	1.13
4	487	1.31	0.93	35.67	19.71	2.46
5	1197	3.23	2.09	87.81	48.52	6.06

Note: Assumes monodisperse particles of unit density and adjusting for inhalability in the rat.

The strong inverse linear relationship ($r^2 = 0.98$) between the clearance of PSPs from the lung and the volume of such particles in the lung is depicted in Figure 14. Morrow (1994) suggests that the mass concentrations in the lung leading to the onset of reduced AM clearance and eventual stasis of 1 and 10 mg per gram of lung, respectively, should be expressed in terms of the volumetric inhibition of AM mobility. This leads to 1000 and 10,000 nL per gram of lung, respectively, as the dust loadings in Figure 14 associated with the onset and eventual stasis of AM mobility. The strength of the relationship between the pulmonary clearance coefficient, k, and the volume of dust in the lung from data pooled across studies in rats that used differing exposure levels of various types of PSP lends strong support to volumetric inhibition of AM as being a unifying concept for the basis of lung overload.

However, data such as contained in Figure 14 do not provide insights as to the biological mechanisms involved, the relative importance of the various alveolar region clearance pathways (Fig. 13), temporal shifts in clearance pathways, or the dose metrics that may be more proximally associated with critical steps in the process of lung overload. Relative to dose metrics, Driscoll (1996) found a strong correlation between the percentage of rats with lung tumors in various PSP studies and the lung burden expressed as the surface area of the particles in square meters per lung. Driscoll (1996) only used the dose levels that yielded statistically significant increases in tumors in his correlation analysis. For Figure 15, Driscoll's surface-area data were used but the tumor data are expressed as the fraction of rats with lung tumors. A logistic curve fit using all data points still demonstrates a strong relationship between the fraction of rats having lung tumors as a function of the surface area of particles per lung. Collectively, the data shown in Figures 14 and 15 establish three principles that are critically important for the carcinogenic risk assessment of PSPs: (1) Substantial lung overload is requisite for induction of lung tumors in rodents; (2) some of the biological mechanisms involved with lung overload are likely not operative at nonoverload exposure levels; and (3) a critical retained lung burden must exist for any given PSP such that exposure levels depicted

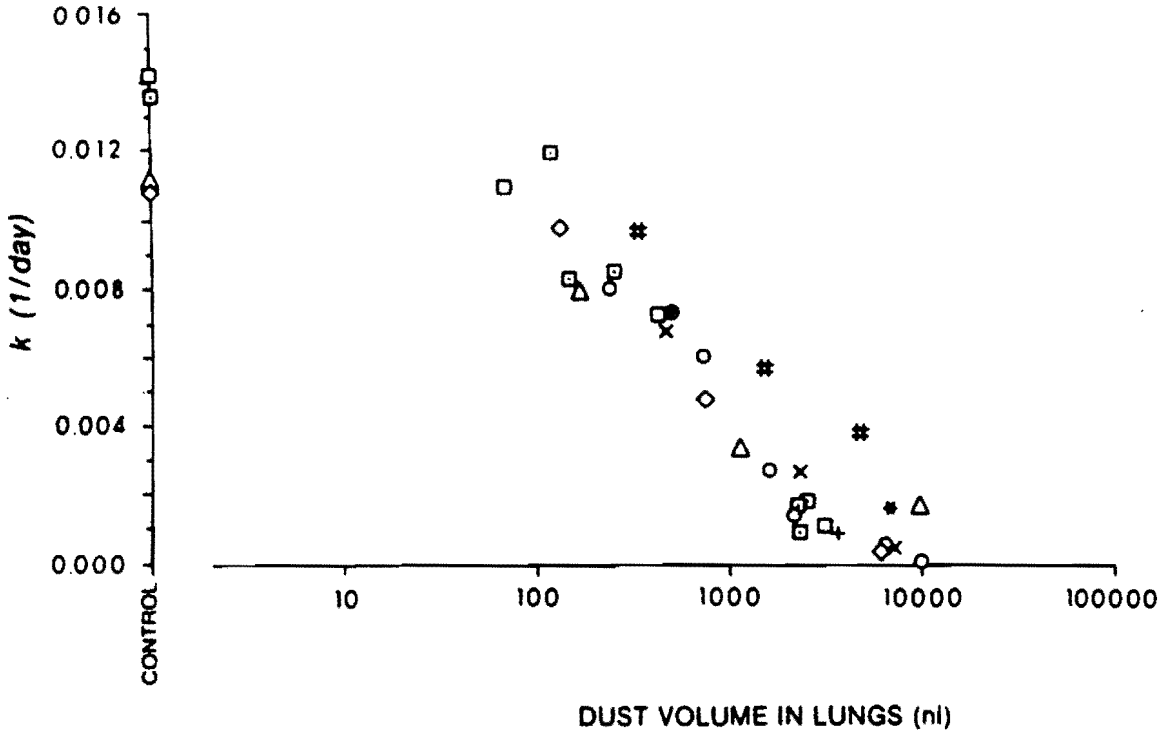

FIG. 14. The pulmonary clearance coefficient, k, is correlated with the retained pulmonary dust volume (nL) and progressively decreases as the particulate volume increases. Data are from the studies indicated: *Square with dot*, toner: Bellmann et al. (1989). *Circle*, toner: Muhle et al. 1990b. *Square, diamond*, and *triangle*, toner: Muhle et al. (1988, 1991). *Plus* and *circled plus*, Titanium dioxide: Muhle et al. (1988, 1990c). *X*, diesel: Heinrich et al. (1986, 1989). *Number sign*, polyvinyl chloride: Muhle et al. (1990a). *Asterisk*, carbon black: Muhle et al. (1990c). From Morrow (1994). Used with permission; copyright 1994 International Life Sciences Institute, Washington, DC.

schematically by curves A and B of Figure 1 can be identified and for which there is essentially no carcinogenic risk.

Given the complex relationships among deposition mechanisms, clearance pathways and kinetics, and morphometric characteristics of various alveolar parameters, the most reasonable approach for understanding lung overload and establishing critical lung burdens associated with this phenomenon involves the use of physiologically based dosimetry models. Such models can incorporate the necessary complexities and help identify experimental studies that could shed light on issues needing resolution and that will enable important model parameters to be estimated. As noted previously, Stöber and colleagues (1989, 1990a, 1990b, 1994) have developed various physiologically based dosimetry models and have used them to advance our understanding of key aspects of lung overload. For example, Stöber and Mauderly (1994) examined the hypothesis that the time integral of the interstitial burden can be used as an effective relative dose for overload carcinogenesis in the rat. They incorporated new data on temporal patterns of lymph node bur-

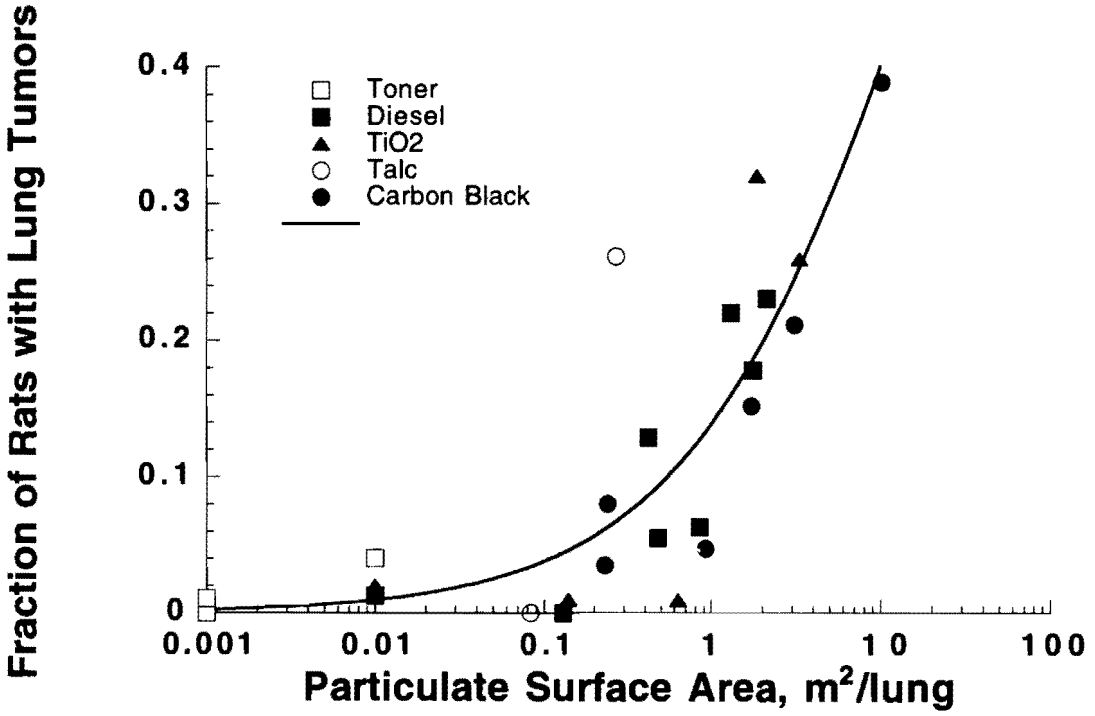

FIG. 15. The fraction of rats with lung tumors after exposure to various poorly soluble particles as a function of the particulate surface area in the lung. The figure is based on data contained in Driscoll (1996). The solid curve represents the fit of a logistic function of the form $y = (1+e^{-(\alpha+\beta \log x)})^{-1}$, where y represents the fraction of rats with lung tumors, and x represents the surface area of the particles in the lung. The fitted values of the parameters α and β are -1.828 and 1.419, respectively; here $R^2 = 0.71$.

dens of PSPs and were able to obtain reasonable fits to the experimental data by adjusting interstitial clearance kinetics. Given the variability in the experimental data, Stöber and Mauderly (1994) categorized their efforts as leading to dose–response interpretations that were better founded on a theoretical basis but that still might be considered as speculative. Nonetheless, although one might have to agree with Morrow (1994) that currently we are only able to speculate on the relative roles of the complex mechanisms and factors leading to lung overload, dosimetry and biologically based dose-response modeling undoubtedly are needed to synthesize our knowledge about lung overload and to identify critical data gaps. Recently, Stöber (1998) illustrated how such models can provide a framework for assessing either constant or variable daily exposure regimens and identifying exposure levels that represent a theoretical no-effect threshold for overload carcinogenesis.

SUMMARY

Despite significant structural differences between laboratory animals and humans in various regions of the respiratory tract, the same major mechanisms for deposi-

tion of particles are operative, although the relative importance of these mechanisms in a given region may differ between laboratory animals and humans. For particles smaller than 0.5 μm in size, the geometric diameter is the key physical property important for deposition; for particles larger than 0.5 μm, the aerodynamic equivalent diameter of the particle is an important aspect of deposition mechanisms, because it takes into account the size, shape, and density of the particle.

Complex interactions among species-specific respiratory-tract anatomy, the route and depth of breathing, and particle-specific physical properties determine the sites of deposition of particles at various locations within the respiratory tract. These interactions also impart significant intersubject variability in experimental studies on the regional respiratory tract deposition of particles in human subjects. Considerably more particulate deposition data are available for humans than for laboratory animals.

Rodent toxicity studies of inhaled particles have focused on particles smaller than 5 μm d_{ae}. Although such particles are completely inhalable by humans, this is not the case for rodents. The significantly decreased probability of rodents being able to inhale particles must be taken into account in estimating exposure scenarios that would be expected to lead to comparable deposits of particles at specific target sites in the lungs of rodents and humans. Such comparisons are further complicated if the human activity pattern of interest includes ventilation levels that result in humans switching to oronasal breathing, because the oral pathway is less efficient than the nasal pathway at removing particles and so the thoracic burden of particles is increased.

Once particles are deposited, the mechanisms available for the clearance and translocation of particles vary among the ET, TB, and alveolar respiratory-tract regions. The specific mechanisms and pathways that are operative at any particular point in time are complex functions of exposure rate and level, particle size, particle number, and current mass loading. Although the same pathways for clearance of particles in laboratory animals appear to be operative in humans, the relative importance of these pathways can vary considerably between animals and humans. Importantly, once any dissolution of particles has been accounted for, mechanical removal by AMs via the mucociliary escalator or the lymphatics is essentially independent of size for particles smaller than 5 μm d_{ae}. Thus, results from a wide variety of poorly soluble particle types and sizes can be used collectively to examine the phenomenon of lung overload.

Relative to issues associated with lung overload, the impairment of AM-mediated clearance of particles is central. The strength of the inverse linear relationship between the pulmonary clearance coefficient and the volume of dust in the lung from data pooled across studies in rats that used different exposure levels of various types of poorly soluble particles lends strong support to volumetric inhibition of AMs as being a unifying concept for the basis of lung overload. Given that rat AMs can have about twice the volume of mouse or hamster AMs and that inhibition of macrophage-mediated particle clearance appears necessary for the development of lung overload, examining various AM-based dose metrics may aid in understanding the

basis for species differences involved in lung overload. Relative to dose metrics in lung overload, the surface area of particles retained per lung appears to have merit.

Given the complex relationships among deposition mechanisms, clearance pathways, and kinetics, physiologically based dosimetry models offer the best avenue for making interspecies comparisons of biologically effective doses of particles. Such models provide a framework for improved characterizations of dose and response in quantitative risk assessments for inhaled particles.

ACKNOWLEDGMENTS

The author wishes to thank Annie Jarabek of the U.S. Environmental Protection Agency for her assistance in obtaining various tables and figures from the chapter on dosimetry of inhaled particles in the agency's *Air Quality Criteria for Particulate Matter* document. The author also expresses appreciation to the authors of that dosimetry chapter for their comprehensive review of the literature; their excellent work enabled the author to cite, extract, or paraphrase information on the findings of various investigators without having to "track down" the original citations.

REFERENCES

Adamson, I. Y. R., and Bowden, D. H. 1978. Adaptive responses of the pulmonary macrophagic system to carbon: II. Morphologic studies. *Lab. Invest.* 38:430–438.

Albert, R. E., Lippmann, M., Peterson Jr., H. T., Berger, J., Sanborn, K., and Bohning, D. 1973. Bronchial deposition and clearance of aerosols. *Arch. Intern. Med.* 131:115–127.

Andersen I., Lundqvist ,G. R., and Proctor, D. F. 1971. Human nasal mucosal function in a controlled climate. *Arch. Environ. Health* 23:408–420.

Anjilvel, S., and Asgharian, B. 1995. A multiple-path model of particle deposition in the rat lung. *Fundam. Appl. Toxicol.* 28:41–50.

Asgharian, B., and Anjilvel, S. 1998. A multiple-path model of fiber deposition in the rat lung. *Toxicol. Sci.* 44:80–86.

Bailey, M. R., Hodgson, A., and Smith, H. 1985. Respiratory tract retention of relatively insoluble particles in rodents. *J. Aerosol Sci.* 16:295–305.

Barry, B. E., Miller, F. J., and Crapo, J. D. 1985. Effects of inhalation of 0. 12 and 0. 25 parts per million ozone on the proximal alveolar region of juvenile and adult rats. *Lab. Invest.* 53:692–704.

Bates, D. V. 1989. *Respiratory function in disease*, 3rd ed., p. 558. Philadelphia: WB Saunders.

Bates, D. V., Macklen, P. T., and Christie, R. V. 1971. *Respiratory function in disease*, 2nd ed., p. 584. Philadelphia: WB Saunders.

Bellmann, B., Muhle, H., Creutzenberg, O., Dasenbrock, C., Kilpper, R., MacKenzie, J. C., Morrow, P., and Mermelstein, R. 1991. Lung clearance and retention of toner, utilizing a tracer technique during a long-term inhalation study in rats. *Fundam. Appl. Toxicol.* 17:300–313.

Bellmann, B., Muhle, H., Creutzenberg, O., Kilpper, R., Morrow, R., and Mermelstein, R. 1989. Reversibility of clearance impairment after subchronic test toner inhalation. *Exp. Pathol.* 37:234–238.

Brody, A. R., Hill, L. H., Adkin, B., Jr., and O'Connor, R. W. 1981. Chrysotile asbestos inhalation in rats: Deposition pattern and reaction of alveolar epithelium and pulmonary macrophages. *Am. Rev. Respir. Dis.* 123:670–679.

Chan, T. L., and Lippmann, M. 1980. Experimental measurements and empirical modelling of the regional deposition of inhaled particles in humans. *Am. Ind. Hyg. Assoc. J.* 41:399–409.

Chang, L. Y., Graham, J. A., Miller, F. J., Ospital, J. J., and Crapo, J. D. 1986. Effects of subchronic inhalation of low levels of nitrogen dioxide. 1. The proximal alveolar region of juvenile and adult rats. *Toxicol. Appl. Pharmacol.* 83:45–61.

Cohen, B. S. 1987. Deposition of ultrafine particles in the human tracheobronchial tree: A determinant of the dose from radon daughters. In *Radon and its decay products*, ed. P. H. Hopke, pp. 475–486. Washington, DC: American Chemical Society.

Cohen, B. S., Susman, R. G., and Lippmann, M. 1990. Ultrafine deposition in a human tracheobronchial cast. *Aerosol Sci. Technol.* 12:1082–1091.

Crapo, J. D., Chang ,Y. L., Miller, F. J., and Mercer, R. R. 1990. Aspects of respiratory tract structure and function important for dosimetry modeling: Interspecies comparisons. In *Principles of route-to-route extrapolation for risk assessment*, eds. J. R. Gerrity and C. J. Henry, pp. 15–32. New York: Elsevier.

Crapo, J. D., Peters-Golden, M., Marsh-Salin, J., and Shelburne, J. S. 1978. Pathologic changes in the lungs of oxygen-adapted rats: A morphometric analysis. *Lab. Invest.* 39:640–653.

Dahl, A. R., Bice, D. E., Hahn, F. F., Henderson, R. F., Mauderly, J. L., Muggenburg, B. A., Pickrell, J. A., Wolff, R. K., and Hobbs, C. H. 1986. *Acute and subchronic toxicity of methylphosphoric difluoride (DF) by inhalation in rats*, CRDC Report, Aberdeen Proving Grounds. Aberdeen Proving Ground, MD: U. S. Army Chemical Research and Development Center.

Davidson, M. R., and Fitz-Gerald, J. M. 1974. Transport of O_2 along a model pathway through the respiratory region of the lung. *Bull. Math. Biol.* 36:275–303.

Driscoll, K. E. 1996. Role of inflammation in the development of rat lung tumors in response to chronic particle exposure. *Inhalation Toxicology* 8(Suppl):139–153.

Egan, M. J., and Nixon, W. 1989. On the relationship between experimental data for total deposition and model calculations: Part II. Application to fine particle deposition in the respiratory tract. *J. Aerosol Sci.* 20:149–156.

Emmett, P. C., Aitken, R. J., and Hannan, W. J. 1982. Measurements of the total and regional deposition of inhaled particles in the human respiratory tract. *J. Aerosol Sci.* 13:549–560.

Felicetti, S. A., Wolff, R. K., and Muggenburg, B. A. 1981. Comparison of tracheal mucous transport in rats, guinea pigs, rabbits, and dogs. *J. Appl. Physiol.* 51:1612–1617.

Finlay, W. F. 1998. Estimating the type of hygroscopic behavior exhibited by aqueous droplets. *J. Aerosol Med.* 11:221–229.

Foord, N., Black, A., and Walsh, M. 1978. Regional deposition of 2. 5–7. 5 μm diameter inhaled particles in healthy male non-smokers. *J. Aerosol Sci.* 9:343–357.

Gehr, P., Schürch, S., Berthaiume, Y., Im Hof, V., and Geiser, M. 1990. Particle retention in airways by surfactant. *J. Aerosol Med.* 3:27–43.

Gerrity, T. R., Lee, P. S., Hass, F. J., Marinelli, A., Werner, P., and Laurenco, R. V. 1979. Calculated deposition of inhaled particles in the airway generations of normal subjects. *J. Appl. Physiol: Respir. Environ. Exerc. Physiol.* 47:867–873.

Getchell, M. L., and Getchell, T. V. 1992. Fine structural aspects of secretion and extrinsic innovation in the olfactory mucosa. *Microsc. Res. Tech.* 23(2):111–127.

Giacomelli-Maltoni, G., Melandri, C., Prodi, V., and Tarroni, G. 1972. Deposition efficiency of monodisperse particles in human respiratory tract. *Am. Ind. Hyg. Assoc. J.* 33:603–610.

Giordano, A. M., and Morrow, P. E. 1972. Chronic low-level nitrogen dioxide exposure and mucociliary clearance. *Arch. Environ. Health* 25:443–449.

Goodman, R. M., Yergin, B. M., Landa, J. F., Golivanaux, M. H., and Sackner, M. A. 1978. Relationship of smoking history and pulmonary function tests to tracheal mucous velocity in nonsmokers, young smokers, ex-smokers, and patients with chronic bronchitis. *Am. Rev. Respir. Dis.* 117: 205–214.

Gore, D. J., and Patrick, G. A. 1982. A quantitative study of the penetration of insoluble particles into the tissue of the conducting airways. *Ann. Occup. Hyg.* 26:149–161.

Greenspan, B. J., Morrow, P. E., and Ferin, J. 1988. Effects of aerosol exposures to cadmium chloride on the clearance of titanium dioxide from the lungs of rats. *Exp. Lung Res.* 14:491–499.

Hadley, J. 1977. Membrane receptors of the alveolar macrophage: Alterations by environmental contaminants. Doctoral dissertation, Duke University, Durham, NC.

Hahn, I., Scherer, P. W., and Mozell, M. M. 1993. Velocity profiles measured for airflow through a large-scale model of the human nasal cavity. *J. Appl. Physiol.* 75:2273–2287.

Harkema, J. R. 1992. Epithelial cells of the nasal passages. In *Comparative biology of the normal lung*, ed. R. A. Parent, pp. 27–36. Boca Raton, FL: CRC Press.

Hastings, L., and Evans, J. E. 1991. Olfactory primary neurons as a route of entry for toxic agents into the CNS. *Neurotoxicology* 12:707–714.

Hatch, G. E. 1992. Comparative biochemistry of airway lining fluid. In *Comparative Biology of the Normal Lung*, ed. R. A. Parent, pp. 617–632. Boca Raton, FL: CRC Press.

Heinrich, U., Fuhst, R., Peters, L., Muhle, H., Dasenbrock, C., and Pott, F. 1989. Comparative long-term animal inhalation studies using various particulate matter objectives, experimental designs, and preliminary results. *Exp. Pathol.* 37:27.

Heinrich, U., Muhle, H., Takenaka, S., Ernst, H., Fuhst, R., Mohr, U., Pott, F., and Stöber, W. 1986. Chronic effects on the respiratory tract of hamsters, mice and rats after long-term inhalation of high concentrations of filtered and unfiltered diesel engine emissions. *J. Appl. Toxicol.* 6:383.

Hilding, A. C. 1963. Phagocytosis, mucous flow, and ciliary action. *Arch. Environ. Health* 6:6779.

Hofmann, W., and Bergmann, R. 1998. Predictions of particle deposition patterns in human and rat airways. *Inhalation Toxicol.* 10:557–583.

Hofmann, W., Bergman, R., and Koblinger, L. 1999. Characterization of local particle deposition patterns in human and rat lungs by different morphometric parameters. *J. Aerosol Sci.* 30:651–667.

Hofmann, W., and Koblinger, L. 1990. Monte Carlo modeling of aerosol deposition in human lungs: Part II. Deposition fractions and their sensitivity to parameter variations. *J. Arerosol Sci.* 21:675–688.

Hofmann, W., and Koblinger, L. 1992. Monte Carlo modeling of aerosol deposition in human lungs: Part III. Comparison with experimental data. *J. Aerosol Sci.* 23:51–63.

Hofmann, W., and Koblinger, L. 1994. Comparison of particle deposition patterns in human and rat lungs. *J. Aerosol Sci.* 25(Suppl. 1):S505–S506.

Hofmann, W., Koblinger, L., and Martonen, T. B. 1989. Structural differences between human and rat lugs: Implications for Monte Carlo modeling of aerosol deposition. *Health Physics* 57(Suppl. 1):41–47.

Horsfield, K., Dart, G., Olson, E., Filley, G. F., and Cumming, G. 1971. Models of the human bronchial tree. *J. Appl. Physiol.* 31:207–217.

Hounam, R. F., Black, A., and Walsh, M. 1971. The deposition of aerosol particles in the nasopharyngeal region of the human respiratory tract. *J. Aerosol Sci.* 2:47–61.

International Commission on Radiological Protection. (1994). Human respiratory tract model for radiological protection: A report of a task group of the International Commission on Radiological Protection. Elsevier Science Ltd, Oxford, United Kingdom (ICRP publication 66; Annals of the ICRP 24:1–3).

Irvani, J., and van As, A. 1972. Mucus transport in the tracheobronchial tree of the normal and bronchitic rat. *J. Pathol.* 106:81–93.

Katsnelson, B. A., Konysheva, L. K., Privalova, L. I., and Morosova, K. I. 1992. Development of a multicompartmental model of the kinetics of quartz dust in the pulmonary region of the lung during chronic inhalation exposures of rats. *Br. J. Ind. Med.* 49:172–181.

Katsnelson, B. A., Konysheva, L. K., Sharapova, N. Y., and Privalova, L. I. 1994. Prediction of the comparative intensity of pneumoconiotic changes by chronic inhalation exposure to dusts of different cytotoxicity by means of a mathematical model. *Occup. Environ. Med.* 51:173–180.

Kimbell, J. S., Gross, E. A., Joyner, D. J., Godo, M. N., and Morgan, K. T. 1993. Application of computational fluid dynamics to regional dosimetry of inhaled by chemicals in the upper respiratory tract of the rat. *Toxicol. Appl. Pharmacol.* 121:253–263.

Koblinger, L., and Hofmann, W. 1985. Analysis of human lung morphometric data for stochastic aerosol deposition calculations. *Phys. Med. Biol.* 30:541–556.

Koblinger, L., and Hofmann, W. 1988. Stochastic morphological model of the rat lung. *Anat. Rec.* 221:533–539.

Koblinger, L., and Hofmann, W. 1990. Monte Carlo modeling of aerosol deposition in human lungs: Part I. Simulation of particle transport in a stochastic lung structure. *J. Aerosol Sci.* 21:661–674.

Koblinger, L., and Hofmann, W. 1995. Aerosol inhalation in the rat lung: Part II. Theoretical predictions of particle deposition patterns. *J. Aerosol Med.* 8:21–32.

Koblinger, L., Hofmann, W., Graham, R. C., and Mercer, R. R. 1995. Aerosol inhalation in the rat lung: Part I. Analysis of the rat acinus morphometry and construction of a stochastic lung model. *J. Aerosol Med.* 8:7–19.

Landahl, H. D., and Tracewell, T. 1949. Penetration of air-borne particles through the human nose II. *J. Ind. Hyg. Toxicol.* 31:55–59.

Lippmann, M. 1970. Deposition and clearance of inhaled particles in the human nose. *Ann. Otol. Rhinol. Laryngol.* 79:519–528.

Lippmann, M. 1977. Regional deposition of particles in the human respiratory tract. In *Handbook of physiology, section 9: Reactions to physical agents*, eds. D. H. K. Lee, H. L. Falk, S. D. Murphy, and S. R. Geiger, pp. 213–232. Bethesda, MD: American Physiological Society.

Luchtel, D. L. 1976. Ultrastructural observations on the mucous layer in pulmonary airways. *J. Cell Biol.* 70:350a.

Luchtel, D. L. 1978. The mucous layer of the trachea and major bronchi in the rat. *Scanning Electron Microscopy* 11:1089–1098.

Märtens, A., and Jacobi, W. 1973. Die In-vivo bestimmung der aerosolteilchen-deposition im atemtrakt bei mund-bzw. nasenatumg [In vivo determination of aerosol particle deposition in the total respiratory tract]. In *Aerosole in physik, medizin und technik,* pp. 117–121. Bad Soden, West Germany: Gesellschaft fur Aerosolforschung.

Martonen, T. B. 1982. Analytical model of hygroscopic particle behavior in human airways. *Bull. Math. Biol.* 44:425–442.

Martonen, T. B. 1983. On the fate of inhaled particles in the human: A comparison of experimental data with theoretical computations based on a symmetric and asymmetric lung. *Bull. Math. Biol.* 45:409–424.

Martonen, T. B., Barnett, A. E., and Miller, F. J. 1985. Ambient sulfate aerosol deposition in man: Modeling the influence of hygroscopicity. *Environ. Health Perspect.* 63:11–24.

Martonen, T. B., and Hofmann, W. 1986. Factors to be considered in a dosimetry model for risk assessment of inhaled particles. *Radiation Protection Dosimetry* 15:225–232.

Martonen, T. B., Yang, Y., and Dolovich, M. 1994. Definition of airway composition within gamma camera images. *J. Thorac. Imaging* 9:188–197.

Martonen, T. B., Yang, Y., Dolovich, M., and Guan, X. 1997. Computer simulations of lung morphologies within planar gamma camera images. *Nucl. Med. Commun.* 18:861–869.

Martonen, T. B., Yang, Y., Hwang, D., and Fleming, J. S. 1994. Mapping the human lung using Delaunay tessellation. *Comp. Biomed. Res.* 27:245–262.

Martonen, T. B., Zhang, Z., and Yang, Y. 1992. Extrapolation modeling of aerosol deposition in human and laboratory rat lungs. *Inhalation Toxicology* 4:303–324.

McClellan, R. O., and Miller, F. J. 1997. An overview of EPA's proposed revision of the particulate matter standard. *CIIT Activities* 17:1–23

Ménache, M. G., Miller, F. J., and Raabe, O. G. 1995. Particle inhalability curves for humans and small laboratory animals. *Ann. Occup. Hyg.* 39:317–328.

Ménache, M. G., Raabe, O. G., and Miller, F. J. 1996. An empirical dosimetry model of aerodynamic particle deposition in the rat respiratory tract. *Inhalation Toxicology* 8:539–578.

Mercer, R. R., Costa, D. L., and Crapo, J. D. 1995. Effects of prolonged exposure to nitric oxide or nitrogen dioxide on the alveolar septa of the adult rat lung. *Lab. Invest.* 73:20–28.

Mercer, R. R., and Crapo, J. D. 1987. Three-dimensional reconstruction of the rat acinus. *J. Appl. Physiol.* 63:785–794.

Mercer, R. R., and Crapo, J. D. 1990. Spatial distribution of collagen and elastin. *J. Appl. Physiol.* 69:756–765.

Mercer, R. R., Russell, M. L., and Crapo, J. D. 1992. Mucous lining layers in human and rat airways. *Am. Rev. Respir. Dis.* 145:355.

Mercer, R. R., Russell, M. L., and Crapo, J. D. 1994. Alveolar septal structure in different species. *J. Appl. Physiol.* 77:1060–1066.

Mercer, R. R., Russell, M. L., Roggli, V. L., and Crapo, J. D. 1994. Cell number and distribution in human and rat airways. *Am. J. Res. Cell Mol. Biol.* 10:613–624.

Mercer, T. T. 1967. On the role of particle size in the dissolution of lung burdens. *Health Physics* 13:1211–1221.

Miller, F. J., Anjilvel, S., Ménache, M. G., Asgharian, B., and Gerrity, T. R. 1995. Dosimetric issues relating to particulate toxicity. *Inhalation Toxicology* 7:615–632.

Miller, F. J., and Kimbell, J. S. 1995. Regional dosimetry of inhaled gases. In *Concepts in inhalation toxicology*, eds. R. O. McClellan and R. F. Henderson, pp. 257–287. Washington, DC: Taylor and Francis.

Miller, F. J., Martonen, T. B., Ménache, M. G., Graham, R. C., Spektor, D. M., and Lippmann, M. 1988. Influence of breathing mode and activity level on the regional deposition of inhaled particles and implications for regulatory standards. *Ann. Occup. Hyg.* 32(Suppl. 1):3–10.

Morgan, K. T., Kimbell, J. S., Monticello, T. M., Patra, A. L., and Fleishman, A. 1991. Studies of inspiratory airflow patterns in the nasal passages of the f-344 rat and rhesus monkey using nasal molds: Relevance to formaldehyde toxicity. *Toxic. Appl. Pharmacol.* 110:223–240.

Morgan, K. T., Patterson, D. L., and Gross, E. A. 1984, Frog palate mucociliary apparatus: Structure, function, and response to formaldehyde gas. *Fundam. Appl. Toxicol.* 4:58–68.

Morgan, K. T., Patterson, D. L., and Gross, E. A. 1986. Responses of the nasal mucociliary apparatus airborne irritants. In *Toxicology of the nasal passages*, ed. C. S. Barrow, pp. 123–133. Washington, DC: Hemisphere Publishing.

Morrow, P. E. 1988. Possible mechanisms to explain dust overloading of the lungs. *Fundam. Appl. Toxic.* 10:369–384.

Morrow, P. E. 1992. Dust overloading of the lungs: Update and appraisal. *Toxic. Appl. Pharmacol.* 113:1–12.

Morrow, P. E. 1994. Mechanisms and significance of particle overload. In *Toxic and carcinogenic effects of solid particles in the respiratory tract,* ILSI Monograph, eds. U. Mohr, D. L. Dungworth, J. L. Mauderly, and G. Oberdörster, pp. 17–25. Washington, DC: ILSI Press.

Moss, O. R., and Kanapilly, G. M. 1980. Dissolution of inhaled aerosols. In *Generation of aerosols*, ed. K. Willeke, pp. 105–124. Ann Arbor, MI: Ann Arbor Publishers.

Muhle, H., Bellmann, B., Creutzenberg, O., Dasenbrock, C., Ernst, H., Kilpper, R., MacKenzie, J. C., Morrow, P., Mohr, U., and Takenaka, S. 1991. Pulmonary response to toner upon chronic inhalation exposure in rats. *Fundam. Appl. Toxic.* 17:280.

Muhle, H., Bellmann, B., Creutzenberg, O., Fuhst, R., Koch, W., Mohr, U., Takenaka, S., Morrow, P., Kilpper, R., MacKenzie, J., and Mermelstein, R. 1990b. Subchronic inhalation study of toner in rats. *Inhalation Toxicology* 2:341–360.

Muhle, H., Bellmann, B., Creutzenberg, O., Heinrich, U., Ketkar, M., and Mermelstein, R. 1990. Dust overloading of the lungs after exposure of rats to particles of low solubility: Comparative studies. *J. Aerosol Sci.* 21:374–377.

Muhle, H., Bellmann, B., Creutzenberg, O., Stöber, W., Kilpper, R., MacKenzie, J., Morrow, P., and Mermelstein, R. 1988. Pulmonary deposition, clearance and retention of test toner, TiO_2 and quartz during a long term inhalation study in rats. *Toxicologist* 8:69.

Muhle, H., Creutzenberg, O., Bellmann, B., Heinrich, U., and Mermelstein, R. 1990. Dust overloading of lungs: Investigations of various materials, species differences, and irreversibility of effects. *J. Aerosol Med.* 3(Suppl. 1):111–128.

National Council for Radiological Protection and Measurements. 1997. *Deposition, retention and dosimetry of inhaled radioactive substances,* NCRP Report No. 125. Bethesda, MD: National Council of Radiation Protection and Measurements.

Niinimaa, V., Cole, P., Mintz, S., and Shephard, R. J. 1981. Oronasal distribution of respiratory airflow. *Res. Physiol.* 43:69–75.

Oberdörster, G., Ferin, J., and Morrow, P. E. 1992. Volumetric loading of alveolar macrophages (AM): A possible basis for AM-mediated particle clearance. *Exp. Lung Res.* 18:87–104.

Pattle, R. E. 1961. The retention of gases and particles in the human nose. In *Proceedings of an International Symposium, March–April 1960*, ed. C. N. Davis, pp. 302–311. New York: Pergamon Press.

Phipps, R. J. 1981. The airway mucociliary system. In *Respiratory physiology III*, ed. J. G. Widdicombe, pp. 213–260. Baltimore, MD: University Park Press.

Proctor, D. F., and Anderson, I., eds. 1982. *The nose, upper airway physiology and the atmospheric environment.* New York: Elsevier Science Publishers.

Raabe, O. G. 1982. Deposition and clearance of inhaled aerosols. In *Mechanisms in respiratory toxicology*, ed. H. Witschi, pp. 27–76. Boca Raton, FL: CRC Press.

Raabe, O. G., Al-Bayati, M. A., Teague, S. V., and Rasolt, A. 1988. Regional deposition of inhaled monodisperse, coarse, and fine aerosol particles in small laboratory animals. *Ann. Occup. Hyg.* 32(Suppl. 1):53–63.

Raabe, O. G., Yeh, H. C., Schum, G. M., and Phalen, R. F. 1976. *Tracheobronchial geometry: Human, dog, rat, hamster,* report LF-53. Albuquerque, NM: Lovelace Foundation.

Rooney, S. A. 1992. Phospholipid composition, biosynthesis, and secretion. In *Comparative biology of the normal lung*, vol. 1, ed. R. A. Parent, pp. 511–544. Boca Raton, FL: CRC Press.

Roy, M. 1989. Lung clearance modeling on the basis of physiological and biological parameters. *Health Physics* 57(suppl 1):255–262.

Rudolf, G. 1975. Deposition von Aerosolteilchen in der Nase [Deposition of aerosol particles in the nose]. Diploma thesis, University Frankfurt/Main, Frankfurt, Federal Republic of Germany.

Rudolf, G., Gebhart, J., Heyder, J., Scheuch, G., and Stahlhofen, W. 1983. Modelling the deposition of aerosol particles in the human respiratory tract. *J. Aerosol Sci.* 14:188–192.

Rudolf, G., Gebhart, J., Heyder, J., Schiller, C. F., and Stahlhofen, W. 1986. An empirical formula describing aerosol deposition in man for any particle size. *J. Aerosol Sci.* 17:350–355.

Rudolf, G., Köbrich, R., and Stahlhofen, W. 1990. Modelling and algebraic formulation of regional aerosol deposition in man. *J. Aerosol Sci.* 21(Suppl. 1):S403–S406.

Rutland, J., and Cole, P. J. 1981. Mucociliary clearance and ciliary beat frequency in cystic fibrosis compared with sinusitis and bronchiectasis. *Thorax* 36:654–658.

Santa Cruz, R., Landa, J., Hirsch, J., and Sackner, M. A. 1974. Tracheal mucous velocity in normal man and patients with obstructive lung disease: Effects of terbutaline. *Am. Rev. Respir. Dis.* 109:458–463.

Scheuch, G., and Stahlhofen, W. 1988. Particle deposition of inhaled aerosol boluses in the upper human airways. *J. Aerosol Med.* 1:29–36.

Schlesinger, R. B. 1985. Comparative deposition of inhaled aerosols in experimental animals and humans: A review. *J. Toxicol. Environ. Health* 15:197–214.

Schlesinger, R. B. 1988. Biological disposition of airborne particles: Basic principles and application to vehicular emissions. In *Air pollution, the automobile, and public health*, eds. A. Y. Watson, R. R. Bates, and D. Kennedy, pp. 239–298. Washington, DC: National Academy Press.

Schlesinger, R. B. 1989. Deposition and clearance of inhaled particles. In *Concepts in inhalation toxicology*, eds. R. O. McClellan and R. F. Henderson, pp. 163–192. Washington, DC: Taylor and Francis.

Schum, M., and Yeh, H. C. 1980. Theoretical evaluation of aerosol deposition in anatomical models of mammalian lung airways. *Bull. Math. Biol.* 42:1–15.

Smith, T. J. 1985. Development and application of a model for estimating alveolar and interstitial dust levels. *Ann. Occup. Hyg.* 29:495–516.

Snipes, M. B. 1989. Long-term retention and clearance of particles inhaled by mammalian species. *Crit. Rev. Toxicol.* 20:175–211.

Snipes, M. B. 1995. Pulmonary retention of particles and fibers: Biokinetics and effects of exposure concentration. In *Concepts in inhalation toxicology*, eds. R. O. McClellan, and R. F. Henderson, pp. 225–255. Washington, DC: Taylor and Francis.

Snipes, M. B., Boecker, B. B., and McClellan, R. O. 1983. Retention of monodisperse or polydisperse aluminosilicate particles inhaled by dogs, rats, and mice. *Toxicol. Appl. Pharmacol.* 69:345–362.

Snipes, M. B., and Clem, M. F. 1981. Retention of microspheres in the rat lung after intratracheal instillation. *Environ. Res.* 24:33–41.

Soderholm, S. C. 1981, October 5–7. Compartmental analysis of diesel particle kinetics in the respiratory system of exposed animals. Presented at Toxicological Effects of Emissions from Diesel Engines, Raleigh, North Carolina.

Soong, T. T., Nicholaides, P., Yu, C. P., and Soong, S. C. 1979. A statistical description of the human tracheobronchial tree geometry. *Respir. Physiol.* 37:161–172.

Stahlhofen, W., Gebhart, J., and Heyder, J. 1980. Experimental determination of the regional deposition of aerosol particles in the human respiratory tract. *Am. Ind. Hyg. Assoc. J.* 41:385–398a.

Stahlhofen, W., Gebhart, J., and Heyder, J. 1981. Biological variability of regional deposition of aerosol particles in the human respiratory tract. *Am. Ind. Hyg. Assoc. J.* 42:348–352.

Stahlhofen, W., Gebhart, J., Heyder, J., and Scheuch, G. 1983. New regional deposition data of the human respiratory tract. *J. Aerosol Sci.* 14:186–188.

Stahlhofen, W., Gebhart, J., Rudolf, G., and Scheuch, G. 1986. Measurement of the lung clearance with pulses of radioactively-labelled aerosols. *Aerosol Sci.* 17:333–336.

Stahlhofen, W., Rudolf, G., and James, A. C. 1989. Intercomparison of experimental regional aerosol deposition data. *J. Aerosol Med.* 2:285–308.

Stanley, P. H., Wilson, R., Greenstone, M. A., Mackay, I. S., and Cole, P. J. 1985. Abnormal nasal mucociliary clearance in patients with rhinitis and its relationship to concomitant chest disease. *Br. J. Dis. Chest* 79:77–82.

Stephens, R. J., Sloan, M. F., Evans, M. J., and Freeman, J. 1974. Early response of lung to low levels of ozone. *Am. J. Pathol.* 74:31–58.

Stöber, W. 1972. Dynamic shape factors of nonspherical aerosol particles. In *Assessment of airborne particles*, eds. T. T. Mercer, P. E. Morrow, and W. Stöber, pp. 249–289. Springfield, IL: Thomas.

Stöber, W., McClellan, R. D., and Morrow, P. E. 1993. Approaches to modeling disposition of inhaled particles and fibers in the lung. In Toxicology of the lung, eds. D. E. Gardner, J. D. Crapo, and R. O. McClellan; pp. 527–601. New York: Raven Press.

Stöber, W., Miller, F. J., and McClellan, R. D. 1998. Requirements for a credible extrapolation model derived from health effects in rats exposed to particulate air pollution: A way to minimize the risks of human risk assessment? *Appl. Occup. Environ. Hyg.* 13(6):421–431.

Stöber, W., and Mauderly, J. L. 1994. Model-inferred hypothesis of a critical dose for overload tumor induction by diesel soot and carbon black. *Inhalation Toxicology* 6:427–457.

Stöber, W., and McClellan, R. O. 1997. Pulmonary retention and clearance of inhaled biopersistent aerosol particles: Data-reducing interpolation models and models of physiologically based systems. A review of recent progress and remaining problems. *Crit. Rev. Toxicol.* 27:539–598.

Stöber, W., Morrow, P. E., and Hoover, M. D. 1989. Compartmental modeling of insoluble particles deposited in the alveolar region of the lung. *Fundam. Appl. Toxicol.* 13:823–842.

Stöber, W., Morrow, P. E., Koch, W., and Morawietz, G. 1994. Alveolar clearance and retention of insoluble particles in rats simulated by a model inferring macrophage particle load distribution. *J. Aerosol Sci.* 25:975–1002.

Stöber, W., Morrow, P. E., and Morawietz, G. 1990a. Alveolar retention and clearance of insoluble particles in rats simulated by a new physiologically-oriented compartmental kinetics model. *Fundam. Appl. Toxicol.* 15:329–349.

Stöber, W., Morrow, P. E., Morawietz, G., Koch, W., and Hoover, M. D. 1990b. Development in modeling alveolar retention of insoluble particles in rats. *J. Aerosol Med.* 3(Suppl. 1):S129-S154

Stone, K. C., Mercer, R. R., Gehr, P., Stockstill, B., and Crapo, J. D. 1992. Allometric relationships of cell numbers and size in the mammalian lung. *Am. J. Res. Cell Mol. Biol.* 6:235–243.

Strom, K. A., Chan, T. L., and Johnston, J. T. 1988. Pulmonary retention of inhaled submicron particles in rats: Diesel exhaust exposures and lung retention model. *Ann. Occup. Hyg.* 32:645–657.

Subramaniam, R. P., Richardson, R. B., Morgan, K. T., Kimbell, J. S., and Guilmette, R. A. 1998. Computational fluid dynamics simulations of inspiratory airflow in the human nose and nasopharynx. *Inhalation Toxicology* 10:91–120.

Takahashi, S., Kubota, Y., and Hatsuno, H. 1992. Effect of size on the movement of latex particles in the respiratory tract following local administration. *Inhalation Toxicology* 4:113–123.

Tang, I. N., and Munkelwitz, H. R. 1977. Aerosol growth studies III: Ammonium bisulfate aerosols in a moist atmosphere. *J. Aerosol Sci.* 8:321–330.

Tran, C. L., Jones, A. D., and Donaldson, K. 1994. Development of a dosimetric model for assessing the health risks associated with inhaling coal mine dusts, report no. TM/94/01, pp. 1–59. Edinburgh, UK: Institute of Occupational Medicine.

Tran, C. L., Jones, A. D., and Donaldson, K. 1995. Mathematical model of phagocytosis and inflammation after the inhalation of quartz at different concentrations. *Scand. J. Work, Environ. Health* 21(Suppl. 2):50–54.

U. S. Environmental Protection Agency. 1996. Dosimetry of inhaled particles in the respiratory tract. In *Air quality criteria for particulate matter,* vol. II, pp. 10-1–10c-24. Research Triangle Park, NC: National Center for Environmental Assessment.

van As, A., and Webster, I. 1972. The organization of ciliary activity and mucus transport in pulmonary airways. *S. Afr. Med. J.* 46:347–350.

van As, A., and Webster, I. 1974. The morphology of mucus in mammalian pulmonary airways. *Environ. Res.* 7:1–12.

van Ree, J. H. L., and van Dishoeck 1962. Some investigations on nasal ciliary activity. *Practica Oto-Rhino-Laryngologica* 24:383–390

Warheit, D. B., Overby, L. H., George, G., and Brody, A. R. 1988. Pulmonary macrophages are attracted to inhaled particles through complement activation. *Exp. Lung Res.* 14:51–66.

Weibel, E. R. 1963. *Morphometry of the human lung*. Berlin: Springer-Verlag, and New York: Academic Press.

Wolff, R. K. 1992. Mucociliary function. In *Comparative biology of the normal lung*, vol. 1, ed. R. A. Parent, pp. 659–680. Boca Raton, FL: CRC Press.

Wolff, R. K., Henderson, R. F., Snipes, M. B., Griffith, W. C., Mauderly, J. L., Cuddihy, R. H., and McClellan, R. O. 1987. Alterations in particle accumulation and clearance in lungs of rats chronically exposed to diesel exhaust. *Fundam. Appl. Toxic.* 9:154–166.

Wolff, R. K., and Muggenburg, B. A. 1979. Comparison of two methods of measuring tracheal mucous clearance in anesthetized beagle dogs. *Am. Rev. Respir. Dis.* 120:137–142.

Xu, G. B., and Yu, C. P. 1987. Deposition of diesel exhaust particles in mammalian lungs: A comparison between particles in a human nasal cast. *Inhalation Toxicology* 1:1–11.

Yeates, D. B., Aspin, N., Levison, H., Jones, M. T., and Bryan, A. C. 1975. Mucociliary tracheal transport rates in man. *J. Appl. Physiol.* 39:487–495.

Yeh, H. C., and Schum, G. M. 1980. Models of human lung airways and their application to inhaled particle deposition. *Bull. Math. Biol.* 42:461–480.

Yeh, H. -C., and Harkema, J. R. 1993. Gross morphometry of airways. In *Toxicology of the lung*, 2nd ed., eds. D. L. Gardner, J. D. Crapo, and R. O. McClellan, pp. 55–79. New York: Raven Press.

Yeh, H. C., Schum, G. M., and Duggan, M. T. 1979. Anatomic models of the tracheobronchial and pulmonary regions of the rat. *Anat. Rec.* 195:483–492.

Yoneda, K. 1976. Mucous blanket of rat bronchus. *Am. Rev. Respir. Dis.* 114:837–842.

Yu, C. P., Dai, Y. T., Boymel, P. M., Zoitos, B. K., Oberdörster, G., and Utell, M. J. 1998. A clearance model of man-made vitreous fibers (MMVFs) in the rat lung. *Inhalation Toxicology* 10:253–274.

Yu, C. P., and Diu, C. K. 1983. Total and regional deposition of inhaled aerosols in humans. *J. Aerosol Sci.* 5:599–609.